Journal of Building Engineering 44 (2021) 103317

Contents lists available at ScienceDirect

Journal of Building Engineering

journal homepage: www.elsevier.com/locate/jobe

Geopolymer concrete with treated recycled aggregates: Macro and microstructural behavior

Edyta Pawluczuk [a,***], Katarzyna Kalinowska-Wichrowska [a], José Ramón Jiménez [b,*,1], José María Fernández-Rodríguez [c,**,1], David Suescum-Morales [b]

[a] Faculty of Civil and Environmental Engineering, Bialystok University of Technology, Poland
[b] Construction Engineering Area, School of Engineering Sciences of Belmez, Universidad de Córdoba, Córdoba, Spain
[c] Inorganic Chemistry Area, School of Engineering Sciences of Belmez, Universidad de Córdoba, Córdoba, Spain

ARTICLE INFO

Keywords:
Geopolymer concrete
Recycled concrete aggregate
Construction and demolition waste
Alkali activation
Interfacial transition zone

ABSTRACT

Geopolymer concrete is a more environmentally friendly alternative than conventional concrete because its production does not need cement. Instead, waste materials such as fly ash, rice husk ash, slag, etc. are used. This research studies the effect of the activator concentration (6–10 M), curing temperature (40–80 °C) and incorporation ratio of thermally and mechanically treated recycled aggregate (0–100%) on changes in the macrostructural properties of geopolymer concrete. All raw materials were previously characterized by thermogravimetric and differential thermal analysis, X-ray fluorescence and X-ray diffraction. Furthermore, a microstructural characterization was carried out on two geopolymer concrete mixes used as reference: one made with a natural aggregate and the other with a treated recycled aggregate. The interfacial transition zone between the treated recycled aggregate/natural aggregate and geopolymer paste was studied using SEM-EDS. A beneficial effect of the treated recycled aggregates on the compressive strength of geopolymer concrete was observed due to formation of silicate hydrated gel (CSH) and calcium aluminate silicate hydrated gel (CASH). However, a slight increase in the water absorption of geopolymer concrete and the mass of peels after 28 freezing and thawing cycles occurred because of the presence of residual porous cement mortar on the treated recycled aggregate surface.

1. Introduction

Cement clinker production is responsible for about 8% of the world's carbon dioxide (CO_2) emissions [1]. Depending on the type of cement, the manufacture of one ton of ordinary Portland cement (OPC) emits between 0.6 and 1 ton of CO_2 [2–7]. Annual OPC production is expected to increase approximately 50% in the 2017–2050 period [8,9]. Geopolymer concrete is an alternative to traditional cement concrete with low CO_2 emission and low energy consumption [10]. Hence the use of geopolymers, which do not use OPC in their mixes, are rapidly growing in the field of concrete technology [11]. There are even researchers who consider this type of concrete as "the next generation of green concrete" [12]. Geopolymers are three-dimensional amorphous to semi-crystalline aluminosilicate materials which can be produced from natural or synthetic aluminosilicate minerals, or industrial aluminosilicate by-products such as fly ash, red mud, slag, metakaolin, perlite, glass, rice husk ash, clay or a combination of them mixed with an alkaline (potassium or sodium hydroxide, potassium/sodium silicate) [13,14].

In general, geopolymer is one of the inorganic polymers. The polymerization requires a considerably quick reaction of silica (Si)-alumina (Al) under alkaline condition which subsequently create a three-dimensional polymeric chain of Si–O–Al–O bonds [15]. Unlike OPC or pozzolanic cements, geopolymer utilizes the polycondensation of silica, alumina and high alkali content to attain compressive strength [16].

* Corresponding author. Área de Ingeniería de la Construcción y Área de Química Inorgánica, Escuela Politécnica Superior de Belmez, Universidad de Córdoba, Avenida de la Universidad s/n, E-14240, Belmez, Córdoba, Spain.
** Corresponding author. Área de Ingeniería de la Construcción y Área de Química Inorgánica, Escuela Politécnica Superior de Belmez, Universidad de Córdoba, Avenida de la Universidad s/n, E-14240, Belmez, Córdoba, Spain.
*** Corresponding author. Faculty of Civil and Environmental Engineering, Bialystok University of Technology, 15-351, Bialystok, Poland.
E-mail addresses: e.pawluczuk@pb.edu.pl (E. Pawluczuk), jrjimenez@uco.es (J.R. Jiménez), um1feroj@uco.es (J.M. Fernández-Rodríguez).
[1] Both contributed equally to this manuscript.

https://doi.org/10.1016/j.jobe.2021.103317
Received 7 May 2021; Received in revised form 11 September 2021; Accepted 11 September 2021
Available online 15 September 2021

Furthermore, geopolymer incorporating OPC develops calcium silicate hydrates (C–S–H) as well as polycondensation of silica and alumina and a high alkali content to attain compressive strength. The following reactions occur during geopolymerization (Eqs. (1) and (2)) [17]:

$$(Si_2O_5Al_2O_2)_n + H_2O + OH^- \rightarrow Si(OH)_4 + Al(OH)^{4-} \quad (1)$$

$$Si(OH)_4 + Al(OH)^{4-} \rightarrow (Si - O - Al - O)_n + 4H_2O \quad (2)$$

Widespread industry adoption of alkali-activated concrete has the potential to positively contribute to environmental sustainability in both the industrial and construction sectors, since it allows reducing carbon emissions and incorporating waste materials in its manufacture [18]. Geopolymer concrete possesses good physical-chemical and mechanical properties, such as relatively high strength, fire and chemical resistance and thermal stability [12,19]. Moreover, geopolymer concrete retains good properties in acid environments, as well as in the presence of salts and sulphates [20–22]. In combination with Portland cement, geopolymer concrete has better durability properties, extremely low shrinkage and relatively higher strength [23]. The increase in the mechanical properties (compressive strength, flexural strength, and splitting tensile strength) up to the third day of curing occurs at an express pace. Although it continues to grow, it does so at a slower rate until 90 days at least [24].

Any material that contains amorphously Si and Al can be used to produce geopolymer concrete. Fly ash and blast furnace slag are the most common waste materials used in geopolymer concrete production [12,18,25–28]. The mixture of fly ash and blast furnace slag improves the pore structure and mechanical strengthof geopolymers compared to the exclusive use of fly ash, this mixture also increases the binder's resistance to the negative effects of acids, sulphates and seawater. Geopolymer properties often depend of the quality of the raw materials used [29]. A significant advantage of using granulated blast furnace slag is that it requires a smaller amount of highly expensive alkaline activator, compared for example to metakaolin, to be activated [30]. However, the use of other waste materials as a partial binder replacement in geopolymer concrete is being sought, to demonstrate that ceramic waste could be also a good source for geopolymer synthesis [31,32].

Construction and demolition waste (CDW) is generated during the construction, useful life, and total or partial demolition phase of buildings or infrastructure. CDW production exceeds 30 billion tons annually worldwide [33–35]. Recycled aggregates (RA) can be obtained from CDW, which is conveniently treated in recycling plants. Countries such as Japan, Germany, and the Netherlands recycle more than 80% of CDW, while other developed countries have a lower recycling rate (Cyprus, Slovenia, and Sweden) [36,37]. According to the Waste Framework Directive (2008/98/EC) of the European Union and the EU Parliament, by 2020, a minimum of 70% of CDW should have been recovered [38,39]. Recycled aggregate (RA) can be classified according to its composition and physical-mechanical properties. Depending on its particle size distribution, RA can be classified as coarse recycled aggregates (4.75–31.5 mm) or fine recycled aggregates (<5 mm). The coarse fraction has been extensively researched for the manufacture of structural [40–45] or non-structural concrete [46–48]. Few research studies have focused on the fine fraction, and most of the studies are focused on low- or high-strength materials [7,49,50]. Recycled concrete aggregates (RCA) are rougher and more porous than natural aggregates (NA); hence, they have a lower particle density and higher water absorption. The presence of microcracks and lower fragmentation resistance is also one of the properties of recycled aggregates; these differences between RCA and NA are mainly due to the attached cement paste. The replacement of NA with RCA in cement-based materials generally reduces its mechanical and durability properties [51].

To improve the physical-mechanical properties of RA, several techniques have been proposed [52]: a) selective demolition and proper treatment of CDWs in recycling plants [53], b) separation of attached mortar from NA [33] with techniques such as mechanical grinding, traditional heating [54–57], microwave heating, and pre-soaking in an acid solution, and c) treatment with CO_2 [7,36,58,59].

A promising alternative recycling option appears to be alkali-activated materials and geopolymer binders, incorporating the RA as either inert aggregates or partially reactive materials [60,61]. It is known that the presence of residual mortar (RM) in recycled concrete aggregates (RCA) can also release some alkalis into pore solution and increase the risk of AAR. Alkali-aggregate reaction (AAR) is affected by many factors such as alkali reactivity of original aggregate (OA), presence of residual mortar (RM) and production procedure. Previous treatments of recycled aggregates to reduce RM is a measure used to mitigate ARR in recycled concrete [62].

Concrete and/or fired clay waste aggregates were studied in several research papers [63–67]. Concrete, brick, glass and ceramic tile waste in geopolymer binders were also investigated by several authors [68–70]. Brick waste aggregates alone were specifically studied in several research papers [71,72]. There are no studies on the influence of the use of treated recycled aggregate from thermal and mechanical treatment in geopolymer concrete. Studies on this topic would complete this gap in knowledge.

The mechanical and physical characterization of metakaolin slag-potassium silicate geopolymers with 40–60% of CDW aggregates, although not exhaustive, provided encouraging results and pointed out interesting aspects related to their possible exploitation as a building material [73]. Concrete and fired clay aggregates determined slightly different results, while a blend of them led to intermediate properties. Mixtures with fired clay, despite their generally greater open porosity, showed performances in line with those with concrete aggregates, but with a higher increment of mechanical strength from 7 to 28 days (18% for fired clay and 9% for concrete, on average), probably related to their residual pozzolanic reactivity.

Pacheco-Torgal et al. (2012) [74] suggest that recycling crushed and ground concrete as an ingredient in geopolymeric binders could provide a solution for recycling a higher percentage of CDW. These authors argue that laboratory prepared samples of concrete using recycled aggregates that successfully reuse up to 100% of waste did not accurately reflect real-world conditions. This was due to the presence of impurities that are found in recycled concrete that can be controlled in the laboratory. However, the mechanical strength of geopolymeric binders was less dependent on aggregate interaction and more on the chemical matrix characteristics of the binder.

Kaniand Allahverdi [75] found that waste bricks were more suitable than waste concrete due to their calcinated alumino-silicate content. Their research results also indicate that the compressive strength of geopolymer concrete produced from the waste bricks rises with increasing Na_2O content.

A recent laboratory study by Arulrajah et al. [76] analyzed the performance of recycled crushed aggregate, crushed brick, and reclaimed asphalt pavement as pavement base/subbase materials through geopolymerization. They found that the mechanical strength, density, and stiffness of the CDW increased with the use of slag (a more active binder). The best results were achieved for RCA, which was found to qualify for use as a base material.

Rakhimova and Rakhimov [77] investigated the influence of a type of alkali activator, percentage of blending material and a type of curing condition on the production of alkali-activated cement produced from ground granulated blast furnace slag (GGBFS) and different types of red clay brick waste. Other researchers have used recycled cement mortar for geopolymers [78]. The results show that cement hydrates in the recycled cement mortar can be activated by alkali to reconstruct new cementitious substances. The recycled cement mortar with a higher original cement/sand ratio yields higher strengths of materials.

This research aims to study the effect of activator concentration (6–10 M), curing temperature (40-80 °C) and treated recycled aggregate

from thermally and mechanically treated concrete content (0–100%) on the physical and mechanical properties of alkali-activated concrete with special emphasis on micro and macrostructural behavior. Due to the availability of fly ash in Poland, this material was used as binder in geopolymer mixtures. A complete characterization of all raw materials used in the tested alkali-activated concrete was carried out by thermogravimetric and differential thermal analysis (TGA/DTA), X-ray fluorescence (XRF) and X-ray diffraction (XRD). Furthermore, a microstructural characterization was carried out on two reference mixes: (i) the first one only made with a natural aggregate and (ii) the second one only made with treated recycled aggregates. In these two series, the interfacial transition zone (ITZ) between the aggregate (treated recycled aggregate/natural aggregate) and geopolymer paste was study using SEM-EDS. The microstructural characterization helps explain what happens on the macroscopic level.

2. Materials and methodology

2.1. Materials

The Fly ash (FA) used was collected from the thermal power plant in Ostrołęka (Poland). The particle density of fly ash was 2.2 g/cm^3. As natural aggregates (NA), a river sand fraction 0–2 mm and a gravel fraction 2–4 mm, 4–8 mm and 8–16 mm respectively were used. The test was carried out using treated recycled aggregates (tRA) from concrete debris (RA) of 4–8 mm and 8–16 mm fractions, which were obtained from thermal and mechanical treatments according to patent PAT.229887 from pre-crushed concrete road curbs with declared concrete class C30/37. The patented process (PAT.229887) is based on four main stages, which in laboratory conditions were carried out in the following way: (i) the concrete waste was crushed in a jaw crusher to a particle size 0/40 mm; (ii) the recycled aggregate obtained in this way was placed in a thermal furnace and heated at 650 °C during 60 min (after this stage partial separation of the cement mortar from the aggregate was observed); (iii) once removed from the furnace, the recycled aggregates was placed in a Los Angeles drum and subjected to the mechanical treatment of constant parameters (500 revolutions, 5 steel balls) in order to finally separate the cement mortar from the coarse aggregate particles; and (iv) the cooled material was sieved through a 4 mm sieve to separate a fine fraction (<4 mm) from a coarse fraction (>4 mm). The coarse aggregate was additionally divided into fractions of 4/8 mm and 8/16 mm. The process of obtaining treated recycled coarse aggregate was similar to the one used by Kalinowska-Wichrowska et al. [57]. These authors showed that the recycled concrete aggregates treated according to the Patent PAT.229887 increases the dry bulk density values between 25 and 35% for the 4/8 mm and 8/16 mm fraction respectively and reduces the water absorption by 55 and 53% for the 4/8 mm and 8/16 mm fraction. Table 1 shows the properties of natural aggregate and treated recycled aggregates used.

The alkali activator used for tests was obtained from a combination of sodium hydroxide (NaOH) in solid form (granules) and sodium water glass (Na_2SiO_3). The NaOH solution was used in different molar concentrations: 6 M, 8 M and 10 M. A total amount of 350 kg/m^3 of precursor (fly ash) was used. The ratio Na_2SiO_3/precursor was 0.428. Such a high amount was due to the fact that no water or superplasticizer was used in the mixture because they significantly reduce the compressive strength of the geopolymer concrete. A total of 50 L of NaOH solution was used in each cubic meter of geopolymer concrete, so the quantity of activator (Na_2SiO_3+NaOH) solution was about 60% by weight of fly ash (211.2 kg/m^3) for series with 6 M NaOH solution. The alkaline activator solution was prepared by mixing Na_2SiO_3 solution and the NaOH solution. Due to the high temperature of the alkali-activating solution (40-80 °C), it was prepared 24 h prior to its use to bring down its temperature to laboratory conditions.

Table 1
Properties of the natural aggregate (NA) and treated recycled aggregate (tRA).

Properties	Unit	Natural aggregate (NA)		Treated recycled aggregate (tRA)	
		4–8 mm	8–16 mm	4–8 mm	8–16 mm
Volume density, ρ_a	g/cm^3	2.64	2.64	2.53	2.59
Volume density in dry state, ρ_{rd}	g/cm^3	2.62	2.62	2.50	2.52
Volume density in saturated surface dry state, ρ_{ssd}	g/cm^3	2.66	2.66	2.57	2.58
Water absorption, WA_{24}	%	1.3	1.0	2.5	1.80
Crushing value, C_V	%	10.4	11.4	13.6	11.8

2.2. Experimental design

Three factors were studied in this research (12 series):(i) X_1 - percentage of treated recycled coarse aggregate fraction 4–8 mm and 8–16 mm. Three substitution ratios by weight of natural aggregate for treated recycled aggregate were tested: 0, 50 and 100%; (ii) X_2 - molar concentration of sodium hydroxide (6, 8 and 10 M). The activator concentrations mentioned above were established based on the trial mixtures made previously. It was found that the use of an activator with a concentration above 10 M was not possible due to the lack of the possibility to vibrate the mixture (fast setting), possibly if the aggregates had been previously presaturated, higher molarities could have been tested; and (iii) X_3 - curing temperature (40, 60 and 80 °C) during 24 h. On the basis of the above-mentioned variables, an experimental plan including 12 research series was established (Sequential Hartley's PS/DS-P:Ha3 plan). Table 2 shows the geopolymer concrete mix proportions and test plan. For X_1 the normalized values were −1 if the percentage of substitution was 0%, 0 for 50% of substitution and 1 for 100% of substitution of NA by tRA. For X_2 the normalized values were −1 if the Molar concentration was 6 M, 0 for 8 M and 1 for 10 M. For $X_3$the normalized values were −1 if the temperature was 40 °C, 0 for 60 °C and 1 for 80 °C. A similar procedure was carried out by Pawluczuk et al. [55].

Series 4 and Series 9 were used as reference mixes containing only natural and treated recycled aggregate, respectively.

Due to the similar density of the recycled aggregate after thermal and mechanical treatment and the natural aggregate (Table 1), the amount of tRA was determined by weight, not by volume. Dry aggregates were weighed and placed in a mixer. The aggregates were used dry instead of presaturated to avoid the risk of the later transfer of water from within the aggregates to the geopolymer concrete matrix, which could alter the concentration of the activator solution (Na2SiO3 + NaOH) in the interfacial transition zone (ITZ) and alter the results. After this time, the activator was added and again mixed for 240 s. The mix was laid in forms in three layers. Each layer was compacted for 60 s using a vibrating table. Samples after molding were covered with foil and left for 24 h under laboratory conditions. After 24 h, the samples were transferred to a laboratory dryer for heating at the temperature according to the experiment plan: 40 °C, 60 °C or 80 °C. To avoid evaporation of water from the samples, the molds in the dryer were covered with foil. Samples were heated for 24 h and then allowed to cool. The samples were then de-molded and placed on the grate over the surface of water. Samples matured in this way until they reached the age of 7 or 28 days, depending on the type of tests performed.

2.3. Research methodology

2.3.1. Physical-mechanical tests of the geopolymer concrete

The physical-mechanical tests of the geopolymer concrete were conducted on 100 × 100 × 100 mm samples. The compressive strength tests after 7 and 28 days were carried out on 6 samples in accordance with standard EN 12390–3 [79]. The test for water absorption (after 28

Table 2
Geopolymer concrete mix proportions for 1 m[c]. Real and normalized values.

Series	Curing temperature	FA	NaOH solution [a]	Na_2SiO_3b[b]	Molarity NaOH[c]	Sand	Natural aggregate			Treated recycled aggregate		Real values			Normalized values		
						0–2	2–4	4–8	8–16	4–8	8–16	X_1, %	X_2, M	X_3, °C	x_1	x_2	x_3
	°C	kg			M	kg											
1	60	350	66.9	150	10	585	167	418	502	0	0	0	10	60	−1	1	0
2	40	350	64.1	150	8	585	167	209	251.5	209	251.5	50	8	40	0	0	−1
3	40	350	66.9	150	10	585	167	0	0	418	502	100	10	40	1	1	−1
4[d]	**80**	**350**	61.1	**150**	**6**	585	167	**418**	**502**	**0**	**0**	**0**	**6**	**80**	**−1**	**−1**	**1**
5	80	350	66.9	150	10	585	167	0	0	418	502	100	10	80	1	1	1
6	60	350	61.1	150	6	585	167	209	251.5	209	251.5	50	6	60	0	−1	0
7	80	350	66.9	150	10	585	167	0	0	418	502	0	10	80	−1	1	1
8	40	350	61.1	150	6	585	167	418	502	0	0	0	6	40	−1	−1	−1
9[e]	**80**	**350**	61.1	**150**	**6**	585	167	**0**	**0**	**418**	**502**	**100**	**6**	**80**	**1**	**−1**	**1**
10	40	350	61.1	150	6	585	167	0	0	418	502	100	6	40	1	−1	−1
11	60	350	64.1	150	8	585	167	0	0	418	502	100	8	60	1	0	0
12	40	350	66.9	150	10	585	167	418	502	0	0	0	10	40	−1	1	−1

[a] Total weight NaOH solution.
[b] Sodium silicate solution R145. Oxide content (SiO_2 + Na_2O): 35–43%. Molar module: 1.6 ÷ 2.6.
[c] A total of 50 L of NaOH solution was used in each cubic meter of geopolymer concrete.
[d] Series 4 used as reference geopolymer concrete only with the natural aggregate.
[e] Series 9 used as reference geopolymer concrete only with the treated recycled aggregate.

days of curing) was performed according to the Polish standard PN-88/B-06250 (*Ordinary concrete*) on 4 samples [80]. According to standard EN 12390–7:2009 [81] dry density testing was carried out on 6 samples for 28 days of curing.

The frost resistance test was carried out in the presence of de-icing salts according to the procedure in UNE-CEN/TS 12390–9:2008 [82] based on the Swedish standard SS 13 72 44 (called the Borås method). This test was performed on 5 samples with dimensions of 150 × 150 × 50 mm in each series. This study consisted in determining the mass of exfoliated material from the upper surface of the previously cut sample after 28 cycles of freezing and thawing in the presence of a 3% sodium chloride solution. Before that, however, the samples were properly prepared by sealing them with rubber foil and silicone and polyurethane foam. Then a 3 mm layer of 3% solution of NaCl was placed on the sample (Fig. 1). One cycle of freezing and thawing lasted 24 h. After 28 cycles of freezing and thawing, peels were collected from the surface of the samples, dried to constant mass and weighed.

Fig. 1. Geopolymer concrete frost resistance test.

The measure of frost resistance was mass loss, which was calculated from formula (1):

$$m_L = \frac{m_p}{A} \tag{3}$$

Where: m_L is the mass loss (kg/m^2); m_p is mass of peels (kg); A is the test surface area, (m^2). The UNE-EN 772–11:2011 [83]standard was used to perform the capillary test of geopolymer samples. Samples were dried to constant mass at 70 ± 5 °C and were placed in a container ensuring access of water to the bottom. The samples were then immersed in water to a height of 5 mm ± 1 mm and mass measurements were made after 1, 3, 6, 24 and 48 h, respectively, while maintaining a constant water level.

The percentage mass increase was calculated according to formula (2):

$$\Delta m(\%) = \left(\frac{m_c - m_d}{m_d}\right)\cdot 100 \tag{4}$$

Where Δm – increase of mass (%); m_c– sample mass moistened by capillary action (g); m_d – mass of dried sample (g).

2.3.2. *Physicochemical and microstructural characterization*

To determine the chemical composition of the raw materials (fly ash, natural aggregate and treated recycled aggregate) and for the two references mixes (Series 4 and 9 at the age of 28 days) X-ray fluorescence (XRF) was performed.

All the raw materials and the reference mixes were characterized with XRD patterns. It was carried out with an instrument with CuKα (λ = 1.54050 Å; 40 Kv; 30 mA). Diffraction patterns were measured between 10° to 70° (2θ°) at a rate of 0.006 2θ°min^{-1}.

The particle size distribution of the finest raw materials (fly ash) was measured using ethanol as a dispersant. The samples were dispersed on an ultrasonic vibrator for 10 min before grains-size analysis. The result shown was the average of three repetitions.

Simultaneous thermogravimetric analysis and differential thermal analysis (TGA/DTA) were carried out for the raw materials and for two mixes used as reference control. TGA/DTA was performed at a heating rate of 5 °C.min^{-1}. The working temperature ranged from ambient temperature to approximately 1000 °C.

The morphology, the composition and the ITZ between the aggregate

and geopolymer binder of two mixes used as reference control (Series 4 and 9) were obtained using a scanning electron microscope (SEM) and Back Scattered Electron (BSE). Small portions of hardened geopolymer concrete were cut and then placed in epoxy resin. After 48 h the samples were subjected to further grinding and polishing to ensure high smooth surface quality. Silicon carbide papers of decreasing grit size were also used. For the mixes a sputtered with carbon was used.

3. Results and discussion

3.1. Physicochemical characterization of raw materials

Table 3 shows the chemical composition of raw materials obtained with X-ray fluorescence (XRF). The largest chemical oxides equivalent composition for fly ash were SiO_2 and Al_2O_3, which was in accordance with other previous characterization studies [13,19,84,85]. The ratio SiO_2/Al_2O_3 was of 1.55. This ratio is slightly lower than the optimal ratio (2.5–3.5) to achieve the best mechanical properties of concrete [13].The NA is fundamentally siliceous; hence the majority oxide was SiO_2 (quartz). The most important oxides in tRA were CaO followed by SiO_2, which is justified by the previous thermal and mechanical treatment (650 °C during 60 min) [57].

Fig. 2 shows XRD patterns obtained for fly ash, natural aggregate and treated recycled aggregate. The fly ash was observed to be an amorphous compound. The mains phases found for the fly ash was quartz (SiO_2) (46–1045) [86] and mullite ($Al_6Si_2O_{13}$) (15–0776) [86]. Magnetite (19–0629) [86], hematite (33–0664) [86] and anhydrite (37–1496) [86] were also found. These results are in agreement with those shown by other authors [27,84,87]. The main phase found for natural aggregate was quartz (SiO_2) (05–0490) [86]. The phases of calcite ($CaCO_3$) (05–0586) [86], dolomite ($CaMg(CO_3)_2$) (11–0078) [86] and albite ($Na(Si_3Al)O_8$) (09–0457) were also found [86]. This result is in line with the XRF obtained (Table 4). A similar result was found by several authors for siliceous natural aggregates [7,88]. For treated recycled aggregate the main phase found was quartz (SiO_2) (05–0490) [86]. The phases of calcite ($CaCO_3$) (05–0586) [86], dolomite ($CaMg(CO_3)_2$) (11–0078) [86] and albite ($Na(Si_3Al)O_8$) (09–0457) [86] were also found. Although the dehydroxylation of portlandite occurs between 400 and 500 °C (thermal treatment of RA [57]), the storage of the material may have resulted in hydration of the lime (calcium oxide) causing portlandite (44–1481) [86] which was identified in the samples tested. Hatrurite (alite) (86–0402) [86] also appears very mildly. Kalinowska-Wichrowska et al. [57] clearly found the hatrurite phase in samples heated to this same temperature. The ettringite phase also appears (41–1451) [86], which indicates that part of the products, such as hatrurite, formed after heat treatment, have been partially hydrated [89,90].

Table 3
XRF chemical composition of the raw materials.

Oxides	Fly ash	Natural aggregate	Treated recycled aggregate
Na_2O	0.77	0.66	0.34
MgO	1.28	0.85	2.31
Al_2O_3	21.35	2.95	5.86
SiO_2	33.27	41.50	24.39
P_2O_5	0.55	0.05	0.28
SO_3	0.46	0.03	1.47
Cl_2O_3	–	–	0.06
K_2O	2.53	1.34	1.09
CaO	1.60	6.28	27.56
TiO_2	0.92	0.06	0.31
Cr_2O_3	0.02	0.03	–
MnO_2	0.05	0.02	0.06
Fe_2O_3	3.66	0.52	1.87
CuO	0.01	–	–
ZnO	0.01	–	–
SrO	0.05	–	0.04
Rb_2O	0.01	–	–
BaO	–	–	–
BALANCE CO_2	33.39	45.68	34.34
TOTAL	100.00	100.00	100.00

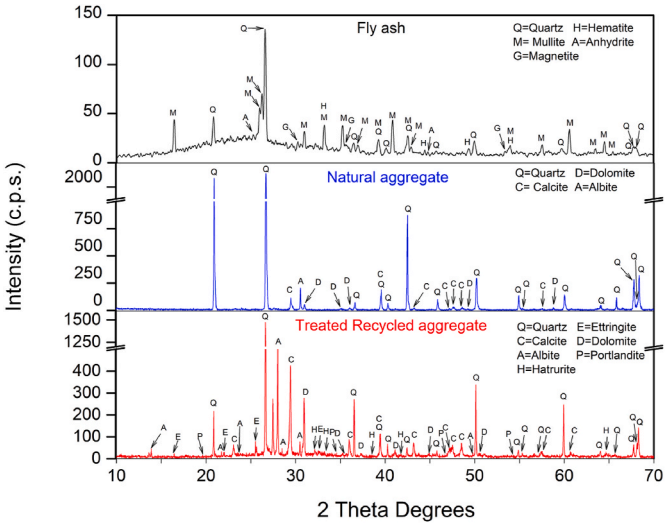

Fig. 2. XRD patterns for the raw materials.

Table 4
XRF chemical composition for reference mixes.

Oxides	Series 4	Series 9
Na_2O	3.36	2.94
MgO	1.06	3.33
Al_2O_3	7.78	8.88
SiO_2	32.95	41.08
P_2O_5	0.17	0.15
SO_3	0.14	0.24
Cl_2O_3	0.02	0.03
K_2O	1.59	1.77
CaO	17.21	11.26
TiO_2	0.26	0.32
Cr_2O_3	0.03	0.05
MnO_2	0.05	0.04
Fe_2O_3	1.79	1.93
SrO	0.03	0.02
BaO	0.05	0.04
BALANCE CO_2	33.56	27.97
TOTAL	100.00	100.00

To know the particle-size distribution of the finest raw materials (fly ash), the particle sizes were measured (Fig. 3). It was observed that fly

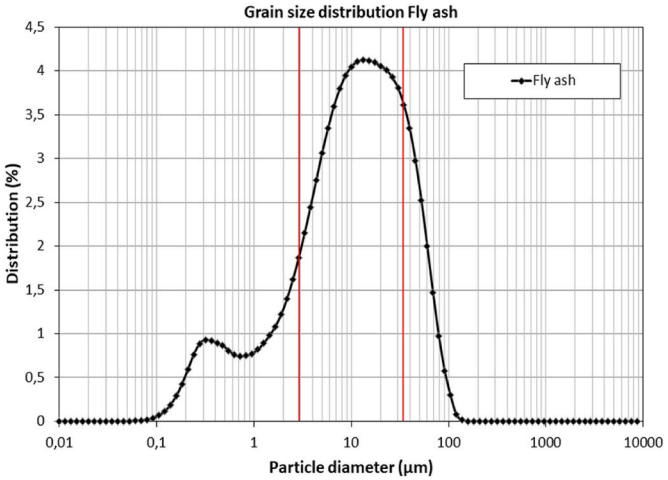

Fig. 3. Grain-size distribution of fly ash measured by laser diffraction.

ash had a wide distribution (from 0.079 to 138.033 μm). A similar result was obtained by Noushini et al. [20] for fly ash. Most of the particles were around 11.5 μm. Assi et al. [91] studied the effect of particle size distribution on the mechanical and microstructural properties of fly ash-based geopolymer concrete. The results show that as particle size decreases, compressive strength increased, the highest value being found for 4.78 μm [91].

Fig. 4 shows the thermogravimetric analysis (TGA, solid line) and differential thermal analysis (DTA, dotted line) for the raw materials. For the fly ash (A) the TGA shows a rapid weight loss associated with an endothermic peak at 40 °C, due to the loss of physically absorbed moisture. From 480 to 700 °C a greater weight loss was observed due to the oxidation and combustion of unburnt coal entrapped inside the fly ash particles [28,92]. For the natural aggregate three stages were observed: from room temperature to 105 °C the humidity contained in the material was lost (0.14%). In the second stage from 105 to 580 °C no weight loss was observed although a peak was found at 573 °C due to the transformation of the quartz from α to β phase (change in crystal structure) [93]. This result is in agreement with the main phase found in XRD for natural aggregate (Fig. 2). From 580 °C (third section), weight loss began to be observed, due to the decomposition of calcite and dolomite. This same behavior was observed by several authors [94,95].

For the treated recycled aggregate three main stages were also observed. The first up to 380 °C, where the observed weight loss occurs due to the loss of humidity and the dehydration of calcium silicates and aluminates [94,96]. In the second stage (380–500 °C) the decomposition of the portlandite found in the XRD occurs (Fig. 2) around 420 °C [94,97,98]. In the third stage (500–1000 °C) at 570 °C a endothermic peak was observed, due to the phase change from quartz α to β phase [93], since it is the main phase found in XRD (Fig. 2). The weight loss observed in this third section was due to the decomposition of calcite and dolomite with a peak around 760 °C [99]. A similar result was found for several authors who used the recycled aggregate [57,100].

3.2. Physicochemical and microstructural characterization of reference mixes

A physicochemical characterization was carried for the two reference mixes: Series 4 and 9. Table 4 shows XRF chemical composition for references mixes. The main oxides for both samples were SiO_2, CaO and Al_2O_3. For Series 4 and 9 an increase in the CaO is striking, compared to what existed in the raw materials (Table 3). This was produced by the activation of the fly ash, whose main phase produced was calcium silicate hydrate with a low Ca/Si ratio (0.79) [8]. In Series 9 an increase in silicon and aluminum was observed, which is due to the formation of aluminosilicate gel in this mixture, as Ren et al. indicated [101].

Fig. 5 shows XRD patterns obtained for the reference mixes. The phases found for Series 4 were quartz (SiO_2) (05–0490) [86], calcite ($CaCO_3$) (05–0586) [86], dolomite ($CaMg(CO_3)_2$) (11–0078) [86] and albite ($Na(Si_3Al)O_8$) (09–0457) [86]. The same phases were found for natural aggregate (Fig. 2) and a small amount of ettringite was also found (41–1451) [[86]. A similar result was found by several authors [21,22,102]. Chindaprasirt et al. [14] indicated that the formation of ettringite occurs from the reaction between anhydrite ($CaSO_4$) (Fig. 2)

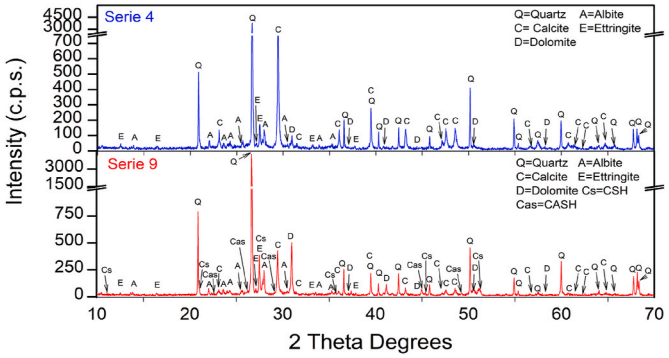

Fig. 5. XRD patterns for Series 4 and 9.

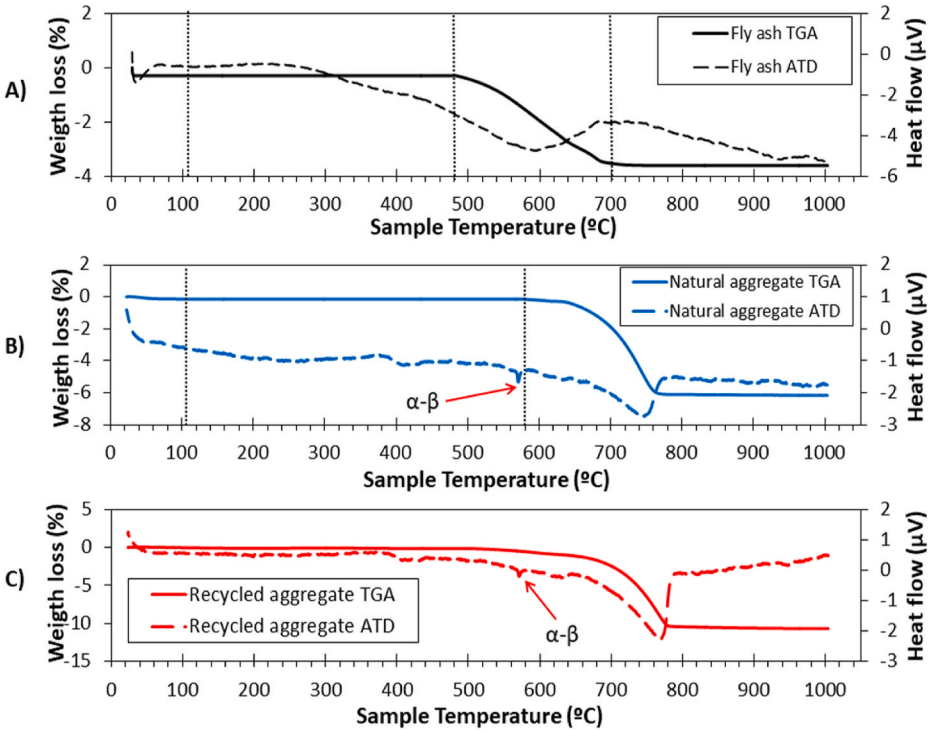

Fig. 4. TGA (solid lines) and DTA (dotted lines) curves: A) for the fly ash, B) for the natural aggregate and C) for the treated recycled aggregate.

and aluminosilicates. This ettringite formation can lead to internal stresses in the geopolymer concrete leading to microcracking. The concentration of alkaline activator Na(OH) (15 M) can prevent the formation of ettringite, which can be negative in excessive amounts for the concrete geopolymer [14]. The main phases found for Series 9 were quartz (SiO_2) (05–0490) [86]. Furthermore, also found were calcite ($CaCO_3$) (05–0586) [86], dolomite ($CaMg(CO_3)_2$) (11–0078) [86] and albite ($Na(Si_3Al)O_8$) (09–0457) [86]. This is in accordance with what was indicated for tRA (Fig. 2), which is the aggregate that is part of this mixture (Series 9). Also, the phases of ettringite (11–0078) [86], xonotlite ($CaSiO_3{\cdot}H_2O$) (03–0341) [86] and calcium aluminum silicate hydrated (52–1344) were found [86]. This result is in agreement with what was found by several authors [102,103] and it was already indicated that these phases could be formed in the analysis of the XRF for Series 9 (Table 4) [101]. The formation of the calcium silicate hydrated gel (CSH) and calcium aluminate silicate hydrated gel (CASH) with the use of RA can result in improved mechanical properties and rapid hardening compared to NA [31,103].

Fig. 6 shows TGA (solid line) and DTA (dotted line) for Series 4 and 9. For Series 4 the TGA can be divided into three stages. In the first stage (from room temperature to 150 °C) a weight loss can be observed attributed to the evaporable water in the concrete geopolymer and to the beginning of decomposition of hydration products, such as ettringite [23,31]. In the second stage (150–500 °C) it was due to the dehydration of calcium silicates and aluminates, no weight loss was observed corresponding to portlandite. In the third section (500–1000 °C) decarbonation of calcite took place [23,31,57,104]. For Series 9 (Fig. 6) a lower weight loss than in Series 4 was observed, which is in accordance with the weight losses found for the NA and tRA (Fig. 4). The same stages as for Series 4 were found; similar results were found by several authors [23,31,57,104].

The interfacial transition zone (ITZ) between the geopolymer binder and aggregates has a very important effect on the mechanical strength of geopolymer concrete, since the weakest point of the concrete with the RA is due to the old attached mortar [8,105]. Most ITZ studies study the two new ITZs formed: one between the RA and geopolymer binder and the other between the NA and geopolymer binder [105]. In this case, only the ITZ between the natural aggregate and the geopolymer binder (for Series 4) and between the treated recycled aggregate and geopolymer binder for Series 9 has been studied.

Fig. 7 shows a SEM image (A) and mapping (B) of Series 4 at low magnification. Unreacted fly ash was first observed, unreacted fly ash particles were also observed by Mehta et al. [21]. Ouda et al. [31] indicated that these unreacted particles reduced the compressive strength of geopolymer structure. Due to the composition shown in the mapping, natural siliceous aggregate (quartz) and some small particles of calcite and dolomite were also observed (Fig. 7 B). Also, microcracks in the geopolymer binder were observed (Fig. 7A) [102]. These microcracks may be due to the process of obtaining the samples (small pieces) or by polishing them [11].

At much higher magnification, even the ettringite can be observed (Fig. 7C and D). This ettringite formation is in line with that already indicated in XRD for Series 4 (Fig. 5) [21,22,102]. Chindaprasirt et al. [14] also found ettringite in geopolymer concrete prepared with NaOH 12 M and lower concentrations (the high concentration of NaOH aids in the dissolution of calcium sulfate and formed calcium hydroxide). For these authors [14,21,22,102] the ettringite was formed in the holes and in microcracks.

Fig. 8 A and B shows a SEM image and mapping of Series 9 at low magnification. The mapping obtained helps to differentiate between the geopolymer binder and the treated recycled aggregate. A microcrack was found in the treated recycled aggregate, which may be due to the previous treatment performed on the RA [57]. Unreacted fly ash was also observed in the geopolymer binder. At this magnification, no microcracks were observed in the binder geopolymer. It appears that the ITZ between the tRA and the geopolymer binder is fully bonded and only small defects appear in some areas that may be due to the polishing process of the samples. At higher magnification (Fig. 8C and D) the zone marked in Fig. 8 B is observed. We can divide the union between the tRA and geopolymer binder into 3 zones: the treated recycled aggregate, ITZ and geopolymer binder. It again appears that the bond between the tRA and geopolymer binder was fully bonded.

A higher magnification was used in Fig. 9. Focusing on the interface area (Fig. 9 A and B) it was observed that the union between interface and geopolymer binder was not fully bonded, having a crack of around 1 μm. At a very high magnification (Fig. 9C and D), in the zone closer to the geopolymer binder, the CSH and CASH gel previously identified by XRD (Fig. 5) could be visualized as an agglomerate of particles.

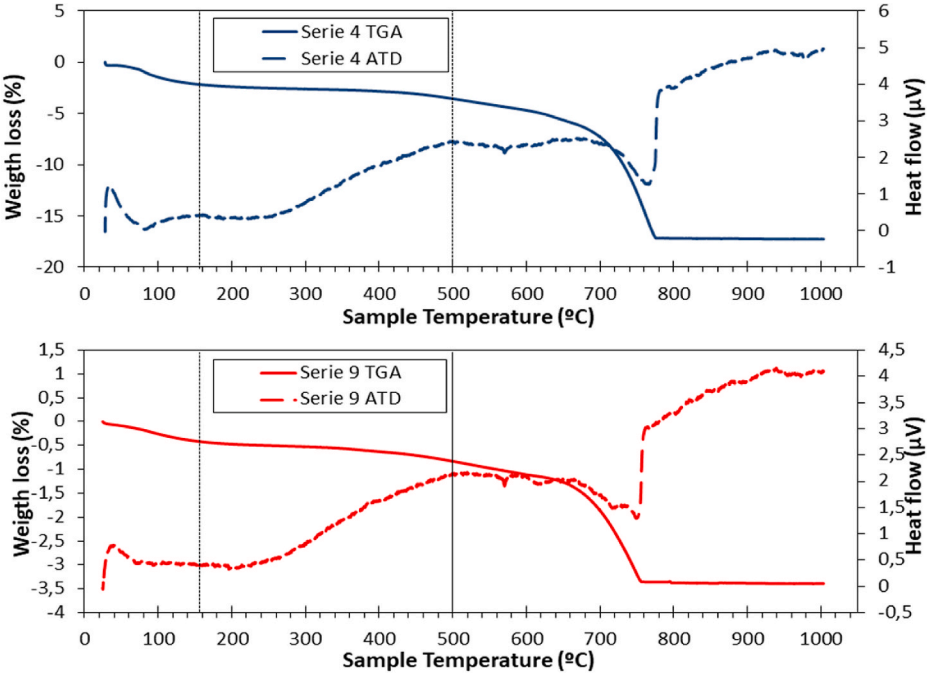

Fig. 6. TGA (solid lines) and DTA (dotted lines) curves for Series 4 and Series 9.

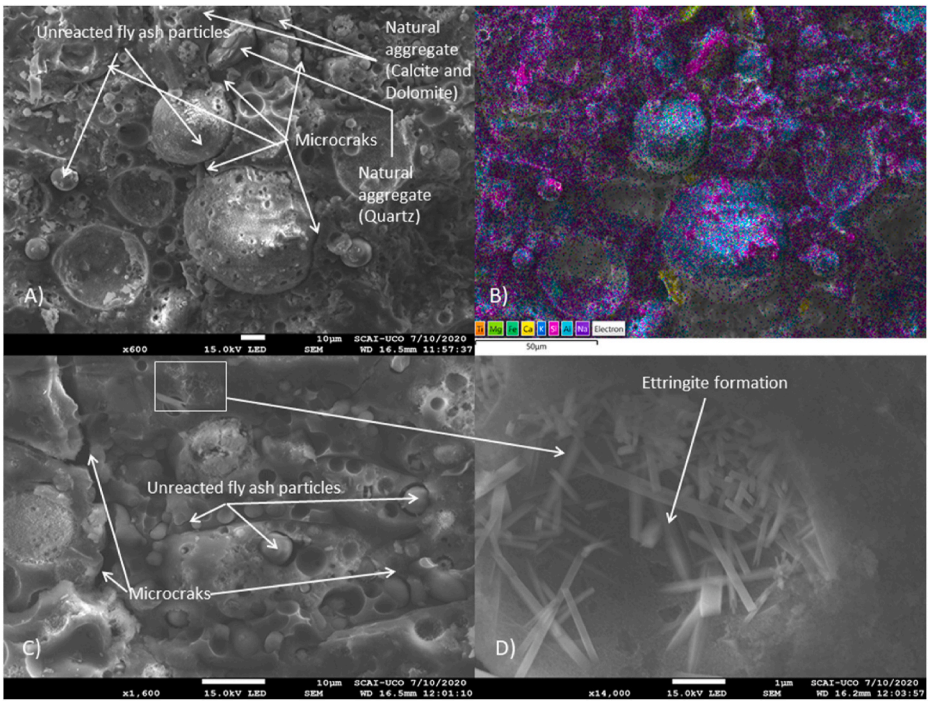

Fig. 7. SEM images and mapping with the identification of the geopolymer binder, natural aggregate and microcracks for Series 4.

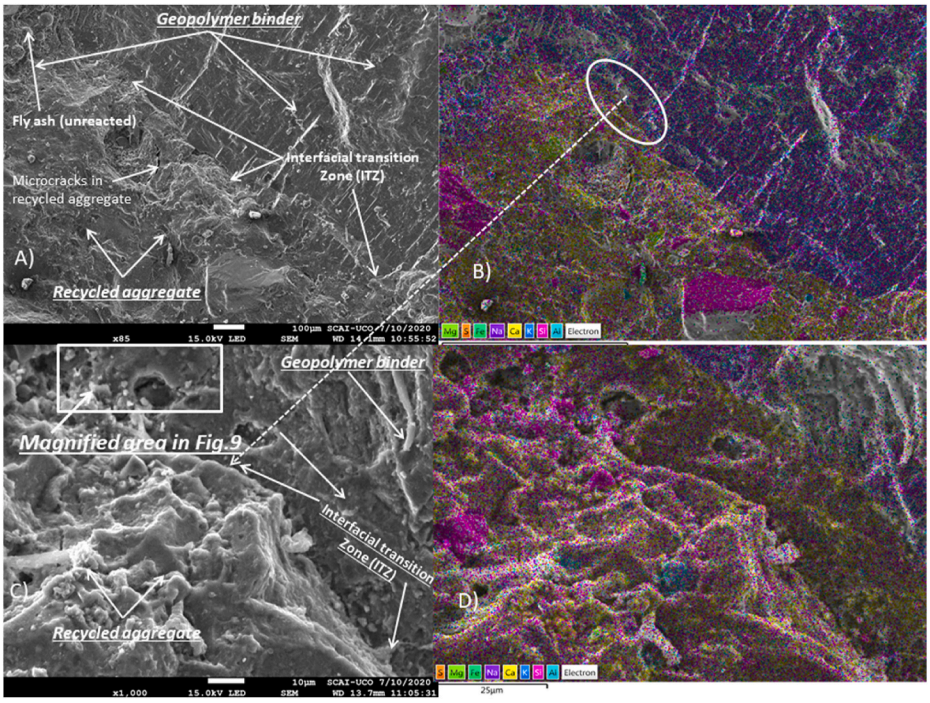

Fig. 8. SEM images and mapping with the identification of unreacted fly ash particles, CSH and CASH formation and microcracks for Series 9.

Additionally, particles of ettringite were observed. Wang et al. [103], using SEM analysis, already indicated that these compounds could be formed. These authors also demonstrated that the curing temperature of 80 °C increased the binding between the RA and the fly ash particles. Xie et al. [29] observed that at the interface between RA and the geopolymer binder aluminosilicate gel (CASH) and CSH gel were formed. Shi et al. [105] found CSH in the ITZ. This formation can lead to an improvement in the mechanical properties [29,31,101,103,105].

3.3. Physical-mechanical properties

Table 5 shows the average test results of the geopolymer concrete in terms of compressive strength after 7 and 28 days, water absorption capacity, water absorption by capillarity, dry density and resistance to freezing and thawing.

The results obtained of geopolymer composite tests were subjected to statistical analysis, aimed at determining the approximating function describing the changes in individual properties of the tested geopolymer

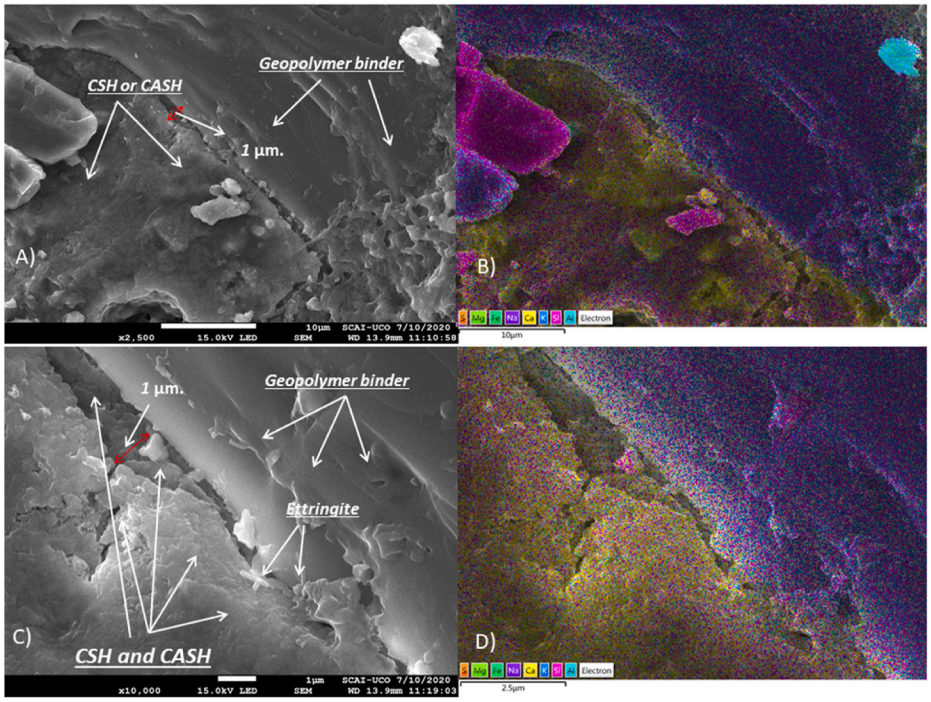

Fig. 9. SEM images and mapping with the identification of the geopolymer binder and the CSH and CASH for Series 9.

Table 5
Average test results of the geopolymer concrete.

Series n°	$f_{cm,7}$	$f_{cm,28}$	Water absorption	Water capillarity	Dry density	Frost resistance
	MPa	MPa	%	%	kg/m^3	kg/m^2
1	41.99	46.94	5.36	5.1	2250	0.84
2	8.77	25.77	5.97	5.7	2210	0.75
3	21.65	36.86	6.34	5.5	2180	0.95
4	37.23	40.19	5.12	4.7	2240	0.00
5	58.95	60.48	5.17	4.3	2250	0.00
6	44.32	47.66	6.35	5.7	2150	0.60
7	47.44	51.48	5.01	4.6	2310	0.00
8	7.74	20.82	7.23	5.7	2120	0.90
9	51.55	52.93	6.86	5.7	2210	0.00
10	12.14	29.47	7.85	6.0	2180	1.23
11	42.00	47.70	6.68	5.9	2190	0.60
12	5.97	22.00	6.86	5.5	2260	0.66

concrete depending on the adopted variable factors (X_1, X_2 and X_3).

The analyses were performed on the values of coded variables ($x_1 = -1$, $x_2 = 0$, $x_3 = 1$). The compressive strength test after 7 days of curing was carried out on 6 samples of 100 × 100 × 100 mm in each series. Figs. 10 and 11 show changes of this feature depending on the variable codes.

Fig. 10 shows that for a curing temperature of 80 °C (x3 = 1) the geopolymer concrete made with 100% of treated recycled concrete aggregate (x1 = 1) and a 10 M activator solution (x2 = 1) reached the highest compressive strength value (Series 5: 58.95 MPa), while the lowest compressive strength value (Series 4: 37.23 MPa) was obtained with the use of 100% natural aggregate (X1 = −1) and a 6 M activator solution (x2 = −1).

Fig. 11 shows that for a 10 M activator solution (x2 = 1) the highest compressive strength value at 7 days (Series 5: 58.95 MPa) was achieved with 100% of coarse treated recycled concrete aggregate (x1 = 1) and a curing temperature of 80 °C (x2 = 1), while the lowest compressive strength value (series 12: 5.97 MPa) was achieved in geopolymer concrete made with 100% of natural aggregate (x1 = −1) and curing temperature of 40 °C (x3 = −1).

From the results analysis (Table 5, Figs. 10 and 11), it was observed

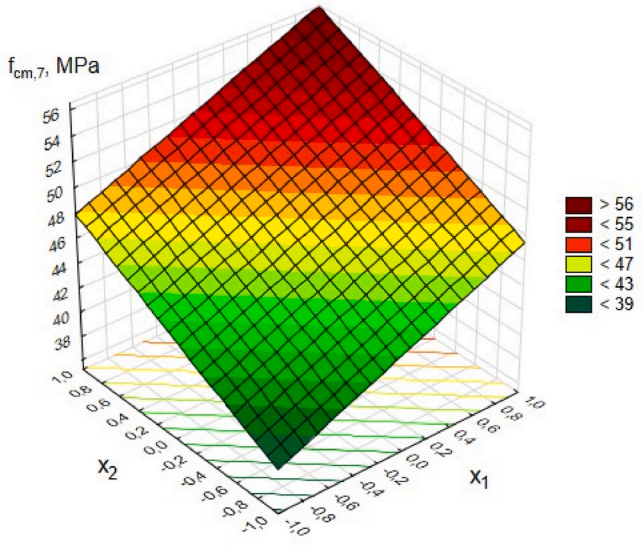

Fig. 10. Compressive strength after 7 days depending on variables x_1 and x_2 with x_3 =1.

that the variable that had the most influence on the compressive strength values was the curing temperature (factor X3). In the case of geopolymer concrete made with a 10 M activator solution and 100% natural aggregate, the compressive strength value increased approximately 695% when the curing temperature increased from 40° to 80 °C (series 12 vs series 7). This increase was lower (172%) in the case of the geopolymer concrete series made with 100% treated recycled concrete aggregate (series 3 vs series 5).

In geopolymer concrete made with 100% natural aggregate, the increase in compressive strength due to the curing temperature was 381% in 6 M solutions (series 8 vs series 4). This value was less than the 695% increase achieved in 10 M solutions (series 12 vs series 7). In geopolymer concrete made with 100% tretaed recycled concrete aggregates, the

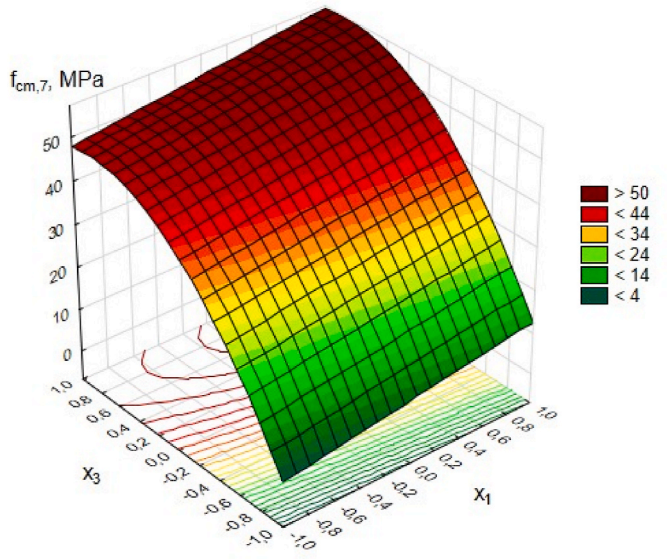

Fig. 11. Compressive strength after 7 days depending on variables x_1 and x_3 with $x_2 = 1$.

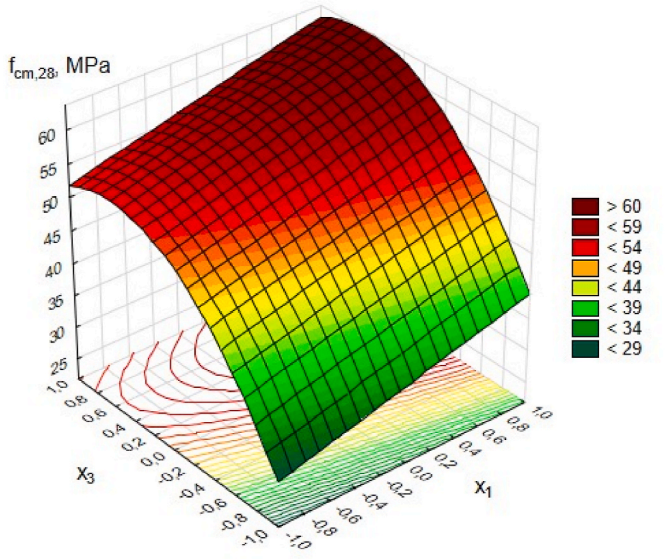

Fig. 13. Compressive strength after 28 days depending on variables x_1 and x_3 with $x_2 = 1$.

increase in compressive strength values was 325% using a 6 M activator solution (series 10 vs series 9) compared to 172% for the 10 M solution (series 3 vs series 5).

The compressive strength test after 28 days was carried out on 6 samples of 100 × 100 × 100 mm in each series. Figs. 12 and 13 show the changes in this feature depending on the variable codes.

In Fig. 12 a trend like Fig. 10 was observed. For a curing temperature of 80 °C (x3 = 1) the geopolymer concrete made with 100% of treated recycled concrete aggregate (x1 = 1) and a 10 M activator solution (x2 = 1) reached the highest compressive strength value (Series 5: 60.48 MPa), while the experimental lowest compressive strength value (Series 4: 40.19 MPa) was obtained with the use of 100% natural aggregate (X1 = −1) and a 6 M activator solution (x2 = −1). Compressive strength values increased only 2.6% in series 5 of geopolymer concrete and 7.95% in series 4, which is much less than in conventional concrete made with OPC.

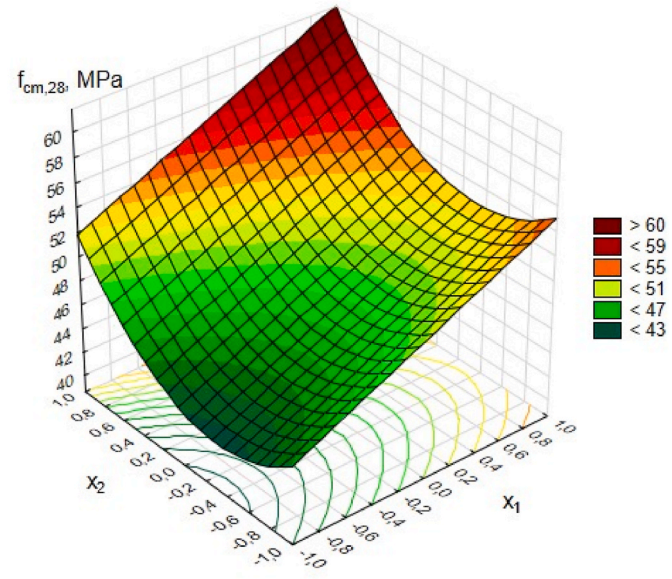

Fig. 12. Compressive strength after 28 days depending on the variables x_1 and x_2 with $x_3 = 1$.

Fig. 13 shows that for a 10 M activator solution (x2 = 1) the highest compressive strength value at 7 days (Series 5: 60.48 MPa) was achieved with 100% of coarse treated recycled concrete aggregate (x1 = 1) and a curing temperature of 80 °C (x2 = 1), while the lowest compressive strength value (series 12: 22.00 MPa) was achieved in geopolymer concrete made with 100% of natural aggregate (x1 = −1) and curing temperature of 40 °C (x3 = −1). However, while the increase in compressive strength values in series 5 was 2.6% from 7 to 28 days of curing age, in series 12 this increase was 269%.

An increase was observed with the use of 100% of treatedrecycled aggregate for a 6 M activator solution and curing temperature of 80 °C (40.19 and 52.93 MPa for Series 4 and Series 9, respectively). This result was in accordance with the new phases (CSH and CASH) found in XRD (Fig. 5) and SEM (Figs. 8 and 9) [29,31,103]. The presence of active cement mortar residue on the surface of the treated recycled aggregate improved the adhesion of the geopolymer mass, thereby improving the strength properties of the composite made with treated recycled concrete aggregates. In addition, calcium oxide remaining after portlandite dehydroxylation because of heating treatment of concrete aggregates (XRF result) actively participated in the polymerization process (Table 4). A high calcium content provides extra nucleation sites for precipitation of dissolved species (CaO), which increases the solidification rate and causes rapid hardening [72].

As in the 7-day analysis, the main factor affecting the 28-day compressive strength values was the curing temperature (factor X3). In the case of geopolymer concrete made with a 10 M activator solution and 100% natural aggregate, the compressive strength value increased approximately 134% when the curing temperature increased from 40° to 80 °C (series 12 vs series 7). This increase was lower (64.1%) in the case of the geopolymer concrete series made with 100% treated recycled concrete aggregate (series 3 vs series 5).

In geopolymer concrete made with 100% natural aggregate, the increase in the compressive strength values due to the curing temperature at the age of 28 days was 93% in 6 M solutions (series 8 vs series 4), a much lower percentage than at 7 days. This value was less than the 134% increase achieved in 10 M solutions (series 12 vs series 7). In geopolymer concrete made with 100% treated recycled concrete aggregates, the increase in the compressive strength values due to the curing temperature was 80% using a 6 M activator solution (series 10 vs series 9) and64% for the 10 M solution (series 3 vs series 5).

Similarly, a beneficial effect of the increase in curing temperature

from 25 °C to 70 °C on the compressive strength of the geopolymer made with recycled material was observed by Allahverdi and Najafi [63]. Hardening in high curing temperature increases compressive strength by removing water from a fresh geopolymer, causing collapse of capillaries with a denser structure [106]. Moreover, the increase in the NaOH concentration clearly influenced the increase in the compressive strength, which is confirmed by the results obtained by other researchers [107,108]. A high NaOH concentration of the system enhanced the leaching of silica and alumina and may have resulted in increased geopolymerization (Eqs. (1) and (2)). The increase in activator concentration has a particularly beneficial effect on the geopolymer composite compressive strength in the presence of a high curing temperature (80 °C). At the curing temperature of 40 °C, after 7 days, only 27–37% of 28-day strength was obtained, when only the natural aggregate was used and 41–59% in the presence of 100% treated recycled aggregate. When the composite was treated at 80 °C after 7 days of curing, it obtained 92% and 97% strength for 28 days, when the natural aggregate and treated recycled aggregate were used respectively.

Thus, the presence of coarse treated recycled aggregate after thermal and mechanical treatment had a very beneficial effect on the strength results of the geopolymer concrete, especially at low curing temperatures. In turn, Nuaklong et al. [109], who also used recycled concrete aggregate for geopolymer concrete based on fly ash, achieved a decrease in the compressive strength by up to 24%. This was due to the fact that the RA was not subjected to any additional treatment and contained approximately 38% of porous cement mortar.

No relationship was found between the dry bulk density and the compressive strength values. The results of the dry bulk density obtained for individual series were in the range of 2120–2310 kg/m^3 and they did not differ from one another by more than 5%.

Figs. 14 and 15 show the trend of water absorption as a function of the variables X_1, X_2 and X_3. The water absorption values of the geopolymer concrete series were affected by all the analyzed factors, although the curing temperature was the most significant. Fig. 14 shows that for a 6 M activator solution (x2 = −1) and a curing temperature of 60 °C (x3 = 0) the highest water absorptionvalue (>6.5%) was achieved with 100% of treated coarse recycled concrete aggregate (x1 = 1), which is justified by the higher water absorption capacity of recycled concrete aggregates [110] and the lowest compressive strength achieved with activator solutions 6 M. The theoretically lowest water absorption value (<4.2%) was achieved in geopolymer concrete made with 50% of natural aggregate and 50% of treated recycled concrete aggregate (x1 = 0),

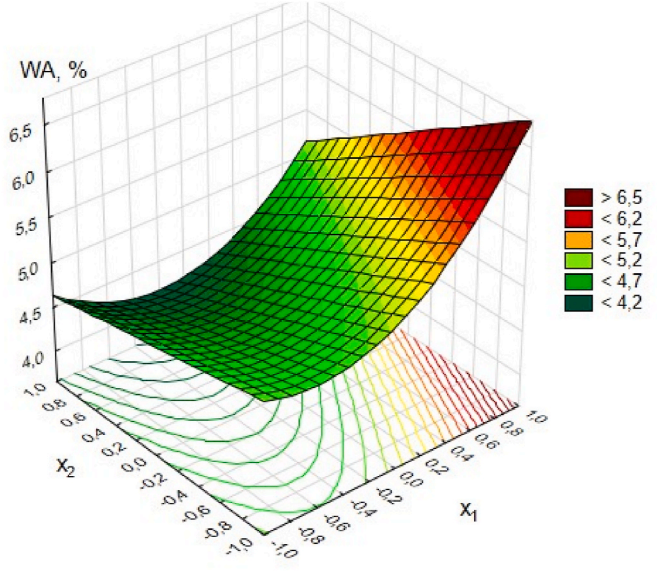

Fig. 14. Water absorption depending on variables x_1 and x_2 with $x_3 = 0$.

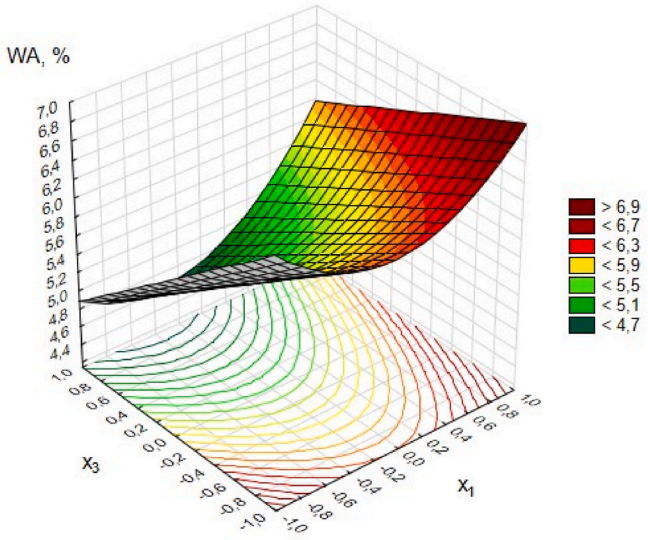

Fig. 15. Water absorption depending on variables x_1 and x_3 with $x_2 = 1$.

which may be justified by the higher compactness capacity of recycled aggregates [111]. The lowest experimental water absorption value (5.36%) obtained for geopolymer concrete cured at 60 °C was obtained for series 1 (x1 = −1; x2 = 1).

Fig. 15 shows that when the curing temperature was lower (x3 = −1) the water absorption increased, especially in geopolymer concrete made with coarse treated recycled concrete aggregates. Series 10 (x1 = 1; x2 = −1; x3 = −1) showed the highest experimental water absorption value (7.85%). In geopolymer concrete made with natural aggregates, when the increase in curing temperature was from 40 °C to 80 °C, a decrease of 29% and 27% in the water absorption values were observed at activator concentrations of 6 M and 10 M, respectively (series 4 vs series 8; series 7 vs series 12). Furthermore, higher activator concentration resulted in a slight decrease in the water absorption by 2% and 5% at a curing temperature of 40 °C and 80 °C, respectively (series 4 vs series 7; series 8 vs series 12).

In geopolymer concrete with 100% treated recycled concrete aggregates the water absorption decreased by 12.6% and 18.5% when the curing temperature increased from 40 °C to 80 °C, at 6 M and 10 M of the activator solution respectively (series 10 vs series 9; series 3 vs series 5).

Fig. 16 shows the evolution over time of the capillarity water absorption after 1, 3, 6, 24 and 48 h of testing. Based on the results of capillarity water absorption, it was found that in the first hour of the test the samples absorbed 20–44% of water regarding the results obtained after 48 h. Samples in Series 4, 5 and 7, with the highest curing temperature, showed the lowest capillarity water absorption values. Curing temperature accelerates the polymerization process and thus seals the composite structure responsible for the water absorption by capillarity. A certain line trend between water absorption by capillarity and water absorption by immersion was observed (Fig. 16 inset).

The geopolymer concrete frost resistance test was performed and the results are shown in Table 5. The weight loss in kg/m^2 was determined based on the mass of peels collected from the surface of samples after 28 freezing and thawing cycles. In series 4, 5, 7 and 9 with the highest curing temperature of 80 °C, no peeling was observed after 28 freezing and thawing cycles. On the contrary, the series with a higher value of weight loss were series 10, 3 and 8, all done with 40 °C. The effect of temperature can be compensated with the increase in the activator concentration (series 8 vs series 12 and series 10 vs series 3). The geopolymer concrete made with AR showed a greater loss of mass than that made with natural aggregates for any temperature, except for 80 °C of curing temperature, and concentration of the activating solution (series 8 vs series 10, series 12 vs series 3). Fig. 17 presents changes in the

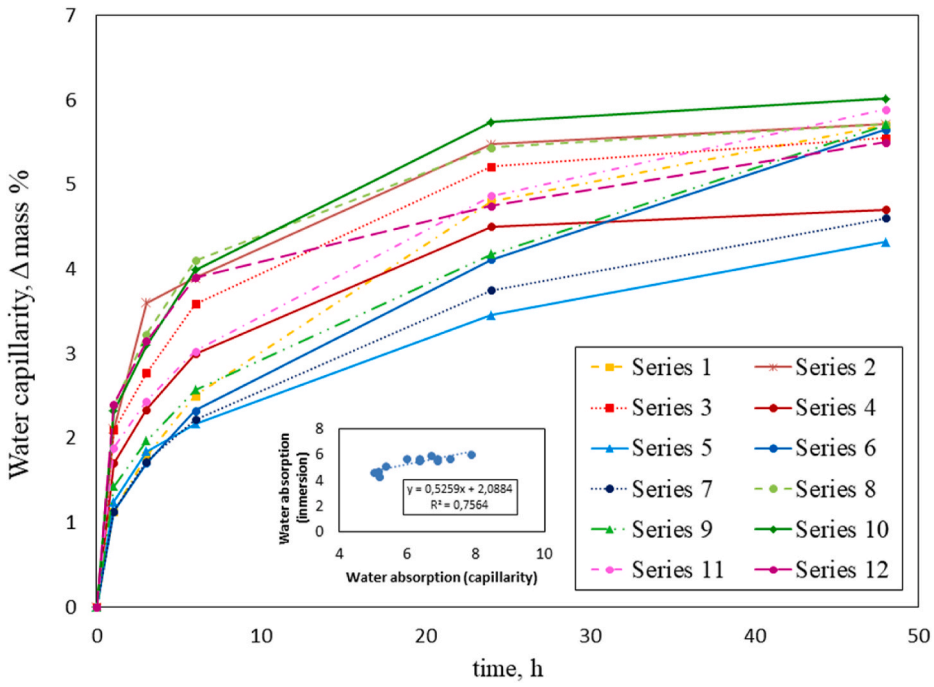

Fig. 16. Water absorption by capillarity over time and relation of water absorption by immersion vs capillarity (inset).

results of frost resistance depending on the content of treated recycled aggregate (x_1) and the curing temperature (x_3).

It can therefore be concluded that the proper curing temperature determines the durability of geopolymer composites. It should be noted that in any series (except Series 10) the mass of peels did not exceed 1.0 kg/m^2, so they can be classified in category FT1 (Mp $\leq$ 1.0 kg/m^2). Different results were obtained by Temuujin et al. [112]. They prepared geopolymer from FA Class F activated by a NaOH/Na_2SiO_3 solution and cured it at 70 °C for 22 h. Their freeze-thaw results showed that these samples had very poor frost resistance, cracking after only 5 cycles.

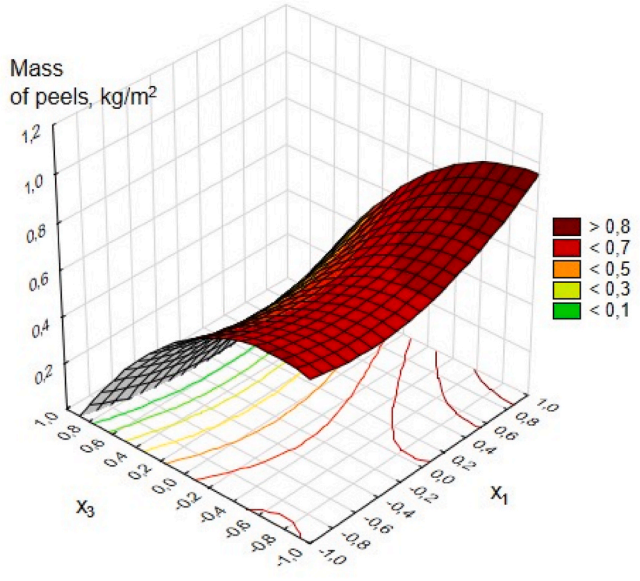

Fig. 17. Weight loss (mass of peels) depending on x_1 and x_3.

4. Short final discussion

The purpose of this work was to determine the impact of molar activator concentration and curing temperature on the properties of geopolymer concrete using natural and thermo-mechanical treated coarse recycled concrete aggregate. Three variables were adopted for the study: X_1 – treated recycled concrete aggregate content (0%, 50%, 100%), X_2-molar activator concentration (6 M, 8 M, 10 M) and X_3 – curing temperature (40 °C, 60 °C, 80 °C). XRD showed that CSH and CASH gel formation when using the treated recycled concrete aggregate in the geopolymer concrete increases the compressive strength and decreases the curing temperature required. By means of SEM, the matrix of the geopolymer concrete with the natural aggregate and treated recycled concrete aggregate was observed. SEM and mapping showed how the CSH and CASH were formed on the interfacial transition zone (ITZ).

Statistical analysis of the test results enabled determining the dependence of the examined features of the geopolymer concrete on the analyzed factors X_1, X_2 and X_3. The substitution of 100% of natural aggregate by thermo-mechanical treated coarse recycled concrete aggregate improved the mechanical properties above all for 6 M activator concentration and 80 °C of curing temperature. This was mainly due to the remains of cement mortar, which resulted in a better connection with the treated recycled concrete aggregate and geopolymer paste (formation of the CSH and CASH on the ITZ). Also, free lime present on the surface of the treated recycled aggregate because of its heating actively participated in the geopolymerization process. However, a slight increase in the absorbability of geopolymer concrete and the mass of peels after 28 freezing and thawing cycles was observed due to the presence of residual porous cement mortar on the tRA surface.

The best geopolymer concrete properties were achieved with a NaOH concentration of 10 M. The highest compressive strength and decrease in water absorption caused by less water supplied to the geopolymer concrete with the activator was observed. Statistically, the parameter with the highest influence on the geopolymer concrete properties was the curing temperature. At 80 °C, the most favorable values for both compressive strength (about a 2-time increase compared to 40 °C) as well as water absorbability (a decrease of 2–3.6%) were measured. Moreover, the lowest water absorption by capillarity and the frost resistance values (no peeling

after 28 cycles) were observed.

5. Conclusion

This paper studied the impact of molar activator concentration and curing temperature on the properties of geopolymer concrete using natural and thermo-mechanical treated coarse recycled concrete aggregate. The results have shown that the presence of the coarse treated recycled concrete aggregate after thermo-mechanical treatment had a very beneficial effect on the mechanical properties of geopolymer concrete, especially at low curing temperatures (40 °C), which, in addition to having a positive effect on the promotion of the circular economy in the construction sector, can have a positive effect on saving energy and reducing carbon emissions in the manufacture of this type of composite materials. As a less favorable factor, it should be noted that the durability properties may be slightly diminished, such as water absorption by immersion, water absorption by capillarity and resistance to freeze-thaw. Further research should be focused on determining the impact of treated recycled concrete aggregates and curing temperature on the durability properties of geopolymer concrete. The best geopolymer concrete properties were achieved with a NaOH concentration of 10 M.

Sample credit author statement

Edyta Pawluczuk and Katarzyna Kalinowska-Wichrowska: conceptualization, methodology, data curation, formal analysis, writing – original draft preparation and funding acquisition; **David Suescum-Morales:** methodology, data curation, formal analysis, writing – original draft preparation; visualization; **José María Fernández and José Ramón Jiménez:** conceptualization, formal analysis, writing-review & editing, supervision and funding acquisition.

Declaration of competing interest

The authors declare that they have no known competing financial interests or personal relationships that could have appeared to influence the work reported in this paper.

Acknowledgments

The study was performed under the research project number WZ/WB-IIL/3/2020 funded by the Polish Ministry of Science and Higher Education. D. Suescum-Morales also acknowledges funding from MECD-Spain (http://www.mecd.-gob.es/educacion-mecd/) FPU 17/04329. The authors would like to acknowledge the financial support from the Ministry of Science and Innovation of the Government of Spain (Ministerio de Ciencia e Innovación del Gobierno de España) through the PRECAST-CO2 research project (Ref. PID2019-111029RB-I00). Funding for open access charge: Universidad de Córdoba / CBUA.

References

[1] J.A.H.W. Olivier, J.G.J. Peters, Trends in Global CO2 and Total Greenhouse Gas Emissions: 2019 Report, PBL, Netherlands Environ. Assess. Agency Hague, Netherlands, 2020.
[2] T. Higuchi, M. Morioka, I. Yoshioka, K. Yokozeki, Development of a new ecological concrete with CO2 emissions below zero, Construct. Build. Mater. 67 (2014) 338–343, https://doi.org/10.1016/j.conbuildmat.2014.01.029.
[3] M.Á. Sanjuán, C. Andrade, P. Mora, A. Zaragoza, Carbon dioxide uptake by mortars and concretes made with Portuguese cements, Appl. Sci. 10 (2020), https://doi.org/10.3390/app10020646.
[4] N. Lippiatt, T.C. Ling, S.Y. Pan, Towards carbon-neutral construction materials: carbonation of cement-based materials and the future perspective, J. Build. Eng. 28 (2020) 101062, https://doi.org/10.1016/j.jobe.2019.101062.
[5] S.K. Kaliyavaradhan, T.-C. Ling, K.H. Mo, CO2 sequestration of fresh concrete slurry waste: optimization of CO2 uptake and feasible use as a potential cement binder, J. CO2 Util. 42 (2020) 101330, https://doi.org/10.1016/j.jcou.2020.101330.
[6] D. Suescum-Morales, D. Cantador-Fernandez, J.M. Fernández, J.R. Jiménez, Potential CO2 capture in one-coat limestone mortar modified with Mg3Al–CO3 calcined hydrotalcites using ultrafast testing technique, Chem. Eng. J. 415 (2021), https://doi.org/10.1016/j.cej.2021.129077.
[7] D. Suescum-Morales, K. Kalinowska-wichrowska, J.M. Fernández, J.R. Jiménez, Accelerated carbonation of fresh cement-based products containing recycled masonry aggregates for CO2 sequestration, J. CO2 Util. 46 (2021), https://doi.org/10.1016/j.jcou.2021.101461.
[8] B. Singh, G. Ishwarya, M. Gupta, S.K. Bhattacharyya, Geopolymer concrete: a review of some recent developments, Construct. Build. Mater. 85 (2015) 78–90, https://doi.org/10.1016/j.conbuildmat.2015.03.036.
[9] D. Suescum-Morales, D. Cantador-Fernández, J.M. Fernández, J.R. Jiménez, Mitigation of CO2 emissions by hydrotalcites of Mg3Al-CO3 at 0 C and high pressure, Appl. Clay Sci. (2020), https://doi.org/10.1016/j.clay.2020.105950.
[10] C. Luan, X. Shi, K. Zhang, N. Utashev, F. Yang, J. Dai, Q. Wang, A mix design method of fly ash geopolymer concrete based on factors analysis, Construct. Build. Mater. 272 (2021) 121612, https://doi.org/10.1016/j.conbuildmat.2020.121612.
[11] J. Temuujin, A. Van Riessen, K.J.D. MacKenzie, Preparation and characterisation of fly ash based geopolymer mortars, Construct. Build. Mater. 24 (2010) 1906–1910, https://doi.org/10.1016/j.conbuildmat.2010.04.012.
[12] M. Amran, S. Debbarma, T. Ozbakkaloglu, Fly ash-based eco-friendly geopolymer concrete: a critical review of the long-term durability properties, Construct. Build. Mater. 270 (2021) 121857, https://doi.org/10.1016/j.conbuildmat.2020.121857.
[13] D. Hardjito, S.E. Wallah, D.M.J. Sumajouw, B.V. Rangan, On the development of fly ash-based geopolymer concrete, ACI Mater. J. 101 (2004) 467–472, https://doi.org/10.14359/13485.
[14] P. Chindaprasirt, S. Thaiwitcharoen, S. Kaewpirom, U. Rattanasak, Controlling ettringite formation in FBC fly ash geopolymer concrete, Cement Concr. Compos. 41 (2013) 24–28, https://doi.org/10.1016/j.cemconcomp.2013.04.009.
[15] C.K. Ma, A.Z. Awang, W. Omar, Structural and material performance of geopolymer concrete: a review, Construct. Build. Mater. 186 (2018) 90–102, https://doi.org/10.1016/j.conbuildmat.2018.07.111.
[16] J. Davidovits, Geopolymers: inorganic polymeric new materials, J. Therm. Anal. Calorim. 37 (1991) 1633–1656, https://doi.org/10.1007/bf01912193.
[17] K.A. Komnitsas, Potential of geopolymer technology towards green buildings and sustainable cities, Procedia Eng 21 (2011) 1023–1032, https://doi.org/10.1016/j.proeng.2011.11.2108.
[18] A. Mohajerani, D. Suter, T. Jeffrey-Bailey, T. Song, A. Arulrajah, S. Horpibulsuk, D. Law, Recycling waste materials in geopolymer concrete, Clean Technol. Environ. Policy 21 (2019) 493–515, https://doi.org/10.1007/s10098-018-01660-2.
[19] Y. Cui, K. Gao, P. Zhang, Experimental and statistical study on mechanical characteristics of geopolymer concrete, Materials 13 (2020), https://doi.org/10.3390/ma13071651.
[20] A. Noushini, A. Castel, J. Aldred, A. Rawal, Chloride diffusion resistance and chloride binding capacity of fly ash-based geopolymer concrete, Cement Concr. Compos. 105 (2020) 103290, https://doi.org/10.1016/j.cemconcomp.2019.04.006.
[21] A. Mehta, R. Siddique, Sulfuric acid resistance of fly ash based geopolymer concrete, Construct. Build. Mater. 146 (2017) 136–143, https://doi.org/10.1016/j.conbuildmat.2017.04.077.
[22] J. Xie, J. Zhao, J. Wang, C. Wang, P. Huang, C. Fang, Sulfate resistance of recycled aggregate concrete with GGBS and fly ash-based geopolymer, Materials 12 (2019), https://doi.org/10.3390/ma12081247.
[23] A.A. Aliabdo, A.E.M. Abd Elmoaty, H.A. Salem, Effect of cement addition, solution resting time and curing characteristics on fly ash based geopolymer concrete performance, Construct. Build. Mater. 123 (2016) 581–593, https://doi.org/10.1016/j.conbuildmat.2016.07.043.
[24] A. Mehta, R. Siddique, Sustainable geopolymer concrete using ground granulated blast furnace slag and rice husk ash: strength and permeability properties, J. Clean. Prod. 205 (2018) 49–57, https://doi.org/10.1016/j.jclepro.2018.08.313.
[25] B.S. Thomas, J. Yang, K.H. Mo, J.A. Abdalla, R.A. Hawileh, E. Ariyachandra, Biomass ashes from agricultural wastes as supplementary cementitious materials or aggregate replacement in cement/geopolymer concrete: a comprehensive review, J. Build. Eng. 40 (2021) 102332, https://doi.org/10.1016/j.jobe.2021.102332.
[26] K. Chen, D. Wu, L. Xia, Q. Cai, Z. Zhang, Geopolymer concrete durability subjected to aggressive environments – a review of influence factors and comparison with ordinary Portland cement, Construct. Build. Mater. 279 (2021) 122496, https://doi.org/10.1016/j.conbuildmat.2021.122496.
[27] J.K. Prusty, B. Pradhan, Multi-response optimization using Taguchi-Grey relational analysis for composition of fly ash-ground granulated blast furnace slag based geopolymer concrete, Construct. Build. Mater. 241 (2020) 118049, https://doi.org/10.1016/j.conbuildmat.2020.118049.
[28] E. Ul Haq, S. Kunjalukkal Padmanabhan, A. Licciulli, Synthesis and characteristics of fly ash and bottom ash based geopolymers-A comparative study, Ceram. Int. 40 (2014) 2965–2971, https://doi.org/10.1016/j.ceramint.2013.10.012.
[29] J. Xie, J. Wang, R. Rao, C. Wang, C. Fang, Effects of combined usage of GGBS and fly ash on workability and mechanical properties of alkali activated geopolymer concrete with recycled aggregate, Compos. B Eng. 164 (2019) 179–190, https://doi.org/10.1016/j.compositesb.2018.11.067.
[30] J. Xie, W. Chen, J. Wang, C. Fang, B. Zhang, F. Liu, Coupling effects of recycled aggregate and GGBS/metakaolin on physicochemical properties of geopolymer

concrete, Construct. Build. Mater. 226 (2019) 345–359, https://doi.org/10.1016/j.conbuildmat.2019.07.311.
[31] A.S. Ouda, M. Gharieb, Development the properties of brick geopolymer pastes using concrete waste incorporating dolomite aggregate, J. Build. Eng. 27 (2020) 100919, https://doi.org/10.1016/j.jobe.2019.100919.
[32] I. Perná, T. Hanzlíček, The solidification of aluminum production waste in geopolymer matrix, J. Clean. Prod. 84 (2014) 657–662, https://doi.org/10.1016/j.jclepro.2014.04.043.
[33] C. Liang, B. Pan, Z. Ma, Z. He, Z. Duan, Utilization of CO2 curing to enhance the properties of recycled aggregate and prepared concrete: a review, Cement Concr. Compos. 105 (2020) 103446, https://doi.org/10.1016/j.cemconcomp.2019.103446.
[34] Y. Li, T. Fu, R. Wang, Y. Li, An assessment of microcracks in the interfacial transition zone of recycled concrete aggregates cured by CO2, Construct. Build. Mater. 236 (2020) 117543, https://doi.org/10.1016/j.conbuildmat.2019.117543.
[35] B.A. Tayeh, D.M. Al Saffar, R. Alyousef, The utilization of recycled aggregate in high performance concrete: a review, J. Mater. Res. Technol. 9 (2020) 8469–8481, https://doi.org/10.1016/j.jmrt.2020.05.126.
[36] V.W.Y. Tam, A. Butera, K.N. Le, W. Li, Utilising CO2 technologies for recycled aggregate concrete: a critical review, Construct. Build. Mater. 250 (2020) 118903, https://doi.org/10.1016/j.conbuildmat.2020.118903.
[37] P. Ghisellini, S. Ulgiati, Economic Assessment of Circular Patterns and Business Models for Reuse and Recycling of Construction and Demolition Waste, Elsevier Ltd., 2020, https://doi.org/10.1016/b978-0-12-819055-5.00003-6.
[38] J. Off, Eur.Union, Directive 2008/56, EC of the European parliament and of the Council, 2008.
[39] J. Tavira, J.R. Jiménez, E.F. Ledesma, A. López-Uceda, J. Ayuso, Real-scale study of a heavy traffic road built with in situ recycled demolition waste, J. Clean. Prod. 248 (2020), https://doi.org/10.1016/j.jclepro.2019.119219.
[40] J. Pacheco, J. de Brito, C. Chastre, L. Evangelista, Experimental investigation on the variability of the main mechanical properties of concrete produced with coarse recycled concrete aggregates, Construct. Build. Mater. 201 (2019) 110–120, https://doi.org/10.1016/j.conbuildmat.2018.12.200.
[41] R.V. Silva, J.R. Jiménez, F. Agrela, J. De Brito, Real-scale applications of recycled aggregate concrete, New Trends Eco-Efficient Recycl. Concr. (2018) 573–589, https://doi.org/10.1016/B978-0-08-102480-5.00021-X.
[42] B. González-Fonteboa, S. Seara-Paz, J. De Brito, I. González-Taboada, F. Martínez-Abella, R. Vasco-Silva, Recycled concrete with coarse recycled aggregate. An overview and analysis, Mater. Construcción 68 (2018) 1–29, https://doi.org/10.3989/mc.2018.13317.
[43] O. Çakir, Experimental analysis of properties of recycled coarse aggregate (RCA) concrete with mineral additives, Construct. Build. Mater. 68 (2014) 17–25, https://doi.org/10.1016/j.conbuildmat.2014.06.032.
[44] M. Amin, B.A. Tayeh, I.S. Agwa, Effect of using mineral admixtures and ceramic wastes as coarse aggregates on properties of ultrahigh-performance concrete, J. Clean. Prod. 273 (2020) 123073, https://doi.org/10.1016/j.jclepro.2020.123073.
[45] M. Abed, R. Nemes, B.A. Tayeh, Properties of self-compacting high-strength concrete containing multiple use of recycled aggregate, J. King Saud Univ. - Eng. Sci. 32 (2020) 108–114, https://doi.org/10.1016/j.jksues.2018.12.002.
[46] A. Lopez-Uceda, J. Ayuso, J.R. Jiménez, A.P. Galvín, I. Del Rey, Feasibility study of roller compacted concrete with recycled aggregates as base layer for light-traffic roads, Road Mater. Pavement Des. 21 (2018) 276–288, https://doi.org/10.1080/14680629.2018.1483257.
[47] A. López-Uceda, J. Ayuso, J.R. Jiménez, F. Agrela, A. Barbudo, J. De Brito, Upscaling the use of mixed recycled aggregates in non-structural low cement concrete, Materials 9 (2016), https://doi.org/10.3390/ma9020091.
[48] A. López-Uceda, J. Ayuso, M. López, J.R. Jimenez, F. Agrela, M.J. Sierra, Properties of non-structural concrete made with mixed recycled aggregates and low cement content, Materials 9 (2016) 1–19, https://doi.org/10.3390/ma9020074.
[49] J. Zhang, J. Wang, X. Li, T. Zhou, Y. Guo, Rapid-hardening controlled low strength materials made of recycled fine aggregate from construction and demolition waste, Construct. Build. Mater. 173 (2018) 81–89, https://doi.org/10.1016/j.conbuildmat.2018.04.023.
[50] J. Tan, J. Cai, X. Li, J. Pan, J. Li, Development of eco-friendly geopolymers with ground mixed recycled aggregates and slag, J. Clean. Prod. 256 (2020) 120369, https://doi.org/10.1016/j.jclepro.2020.120369.
[51] M. Arafa, B.A. Tayeh, M. Alqedra, S. Shihada, H. Hanoona, Investigating the effect of sulfate attack on compressive strength of recycled aggregate concrete, J. Eng. Res. Technol. JERT. 4 (2017) 137–143.
[52] R. Wang, N. Yu, Y. Li, Methods for improving the microstructure of recycled concrete aggregate: a review, Construct. Build. Mater. 242 (2020) 118164, https://doi.org/10.1016/j.conbuildmat.2020.118164.
[53] E.C.D.-G. Environment, EU construction & demolition waste management protocol, Off. J. Eur. Union (2016) 1–22, https://doi.org/10.3390/su11133638.
[54] K. Kalinowska-Wichrowska, D. Suescum-Morales, The experimental study of the utilization of recycling aggregate from the demolition of elements of a reinforced concrete hall, Sustain. Times 12 (2020), https://doi.org/10.3390/su12125182.
[55] E. Pawluczuk, K. Kalinowska-Wichrowska, M. Bołtryk, J.R. Jiménez, J. M. Fernández, The influence of heat and mechanical treatment of concrete rubble on the properties of recycled aggregate concrete, Materials 12 (2019), https://doi.org/10.3390/ma12030367.
[56] K. Kalinowska-Wichrowska, M. Kosior-Kazberuk, E. Pawluczuk, The properties of composites with recycled cement mortar used as a supplementary cementitious material, Materials 13 (2020) 64, https://doi.org/10.3390/ma13010064.
[57] K. Kalinowska-Wichrowska, E. Pawluczuk, M. Bołtryk, Waste-free technology for recycling concrete rubble, Construct. Build. Mater. 234 (2020) 117407, https://doi.org/10.1016/j.conbuildmat.2019.117407.
[58] V.W.Y. Tam, M. Soomro, A.C.J. Evangelista, A review of recycled aggregate in concrete applications (2000–2017), Construct. Build. Mater. 172 (2018) 272–292, https://doi.org/10.1016/j.conbuildmat.2018.03.240.
[59] S.K. Kaliyavaradhan, T.C. Ling, Potential of CO2 sequestration through construction and demolition (C&D) waste - an overview, J. CO2 Util. 20 (2017) 234–242, https://doi.org/10.1016/j.jcou.2017.05.014.
[60] V. Sata, A. Wongsa, P. Chindaprasirt, Properties of pervious geopolymer concrete using recycled aggregates, Construct. Build. Mater. 42 (2013) 33–39, https://doi.org/10.1016/j.conbuildmat.2012.12.046.
[61] S. Mesgari, A. Akbarnezhad, J.Z. Xiao, Recycled geopolymer aggregates as coarse aggregates for Portland cement concrete and geopolymer concrete: effects on mechanical properties, Construct. Build. Mater. 236 (2020) 117571, https://doi.org/10.1016/j.conbuildmat.2019.117571.
[62] Z. Peng, C. Shi, Z. Shi, B. Lu, S. Wan, Z. Zhang, J. Chang, T. Zhang, Alkali-aggregate reaction in recycled aggregate concrete, J. Clean. Prod. 255 (2020) 120238, https://doi.org/10.1016/j.jclepro.2020.120238.
[63] A. Allahverdi, E.N. Kani, Use of construction and demolition waste (CDW) for alkali-activated or geopolymer cements, in: Handb. Recycl. Concr. Demolition Waste, Elsevier Inc., 2013, pp. 439–475, https://doi.org/10.1533/9780857096906.3.439.
[64] V. Sata, P. Chindaprasirt, Use of construction and demolition waste (CDW) for alkali-activated or geopolymer concrete, in: Adv. Constr. Demolition Waste Recycl., Elsevier, 2020, pp. 385–403, https://doi.org/10.1016/b978-0-12-819055-5.00019-x.
[65] A. Vásquez, V. Cárdenas, R.A. Robayo, R.M. de Gutiérrez, Geopolymer based on concrete demolition waste, Adv. Powder Technol. 27 (2016) 1173–1179, https://doi.org/10.1016/j.apt.2016.03.029.
[66] S. Ahmari, X. Ren, V. Toufigh, L. Zhang, Production of geopolymeric binder from blended waste concrete powder and fly ash, Construct. Build. Mater. 35 (2012) 718–729, https://doi.org/10.1016/j.conbuildmat.2012.04.044.
[67] M.F. Zawrah, R.A. Gado, N. Feltin, S. Ducourtieux, L. Devoille, Recycling and utilization assessment of waste fired clay bricks (Grog) with granulated blast-furnace slag for geopolymer production, Process Saf. Environ. Protect. 103 (2016) 237–251, https://doi.org/10.1016/j.psep.2016.08.001.
[68] R.A. Robayo-Salazar, J.F. Rivera, R. Mejía de Gutiérrez, Alkali-activated building materials made with recycled construction and demolition wastes, Construct. Build. Mater. 149 (2017) 130–138, https://doi.org/10.1016/j.conbuildmat.2017.05.122.
[69] D. Zaharaki, M. Galetakis, K. Komnitsas, Valorization of construction and demolition (C&D) and industrial wastes through alkali activation, Construct. Build. Mater. 121 (2016) 686–693, https://doi.org/10.1016/j.conbuildmat.2016.06.051.
[70] K. Komnitsas, D. Zaharaki, A. Vlachou, G. Bartzas, M. Galetakis, Effect of synthesis parameters on the quality of construction and demolition wastes (CDW) geopolymers, Adv. Powder Technol. 26 (2015) 368–376, https://doi.org/10.1016/j.apt.2014.11.012.
[71] R.A. Robayo-Salazar, J.M. Mejía-Arcila, R. Mejía de Gutiérrez, Eco-efficient alkali-activated cement based on red clay brick wastes suitable for the manufacturing of building materials, J. Clean. Prod. 166 (2017) 242–252, https://doi.org/10.1016/j.jclepro.2017.07.243.
[72] L. Reig, M.M. Tashima, M.V. Borrachero, J. Monzó, C.R. Cheeseman, J. Payá, Properties and microstructure of alkali-activated red clay brick waste, Construct. Build. Mater. 43 (2013) 98–106, https://doi.org/10.1016/j.conbuildmat.2013.01.031.
[73] M. Panizza, M. Natali, E. Garbin, S. Tamburini, M. Secco, Assessment of geopolymers with Construction and Demolition Waste (CDW) aggregates as a building material, Construct. Build. Mater. 181 (2018) 119–133, https://doi.org/10.1016/j.conbuildmat.2018.06.018.
[74] F. Pacheco-Torgal, Z. Abdollahnejad, S. Miraldo, S. Baklouti, Y. Ding, An overview on the potential of geopolymers for concrete infrastructure rehabilitation, Construct. Build. Mater. 36 (2012) 1053–1058, https://doi.org/10.1016/j.conbuildmat.2012.07.003.
[75] E.N. Kani, A. Allahverdi, Effect of chemical composition on basic engineering properties of inorganic polymeric binder based on natural pozzolan, Ceram. - Silikaty. 53 (2009) 195–204.
[76] A. Arulrajah, A. Mohammadinia, I. Phummiphan, S. Horpibulsuk, W. Samingthong, Stabilization of recycled demolition aggregates by geopolymers comprising calcium carbide residue, fly ash and slag precursors, Construct. Build. Mater. 114 (2016) 864–873, https://doi.org/10.1016/j.conbuildmat.2016.03.150.
[77] N.R. Rakhimova, R.Z. Rakhimov, Alkali-activated cements and mortars based on blast furnace slag and red clay brick waste, Mater. Des. 85 (2015) 324–331, https://doi.org/10.1016/j.matdes.2015.06.182.
[78] Y.F. Gong, Y.H. Fang, Y.R. Yan, L.Q. Chen, Investigation on alkali activated recycled cement mortar powder cementitious material, Mater. Res. Innovat. 18 (2014) S2784, https://doi.org/10.1179/1432891714Z.000000000477. –S2787.
[79] EN-12390-3, Testing Hardened Concrete. Part 3: Compressive Strength of Test Specimens, AENOR, 2009, 2009.
[80] Polish Standard PN-88/B-06250 (Ordinary Concrete), Concrete Water Absorption Test, 1988.

[81] EN-12390-7:2009, Testing Hardened Concrete. Part 7: Density of Hardened Concrete, 2009.
[82] UNE-CEN/TS 12390-9, Testing Hardened Concrete. Part 9: Freeze-Thaw Resistance, Scaling, 2008, 2008.
[83] UNE-EN 772-11, Determination of Water Absorption of Aggregate Concrete, Autoclaved Aerated Concrete, Manufactured Stone and Natural Stone Masonry Units Due to Capillary Action and the Initial Rate of Water Absorption of Clay Masonry Units, 2011, 2011.
[84] I. Majchrzak-Kucęba, W. Nowak, Characterization of MCM-41 mesoporous materials derived from polish fly ashes, Int. J. Miner. Process. 101 (2011) 100–111, https://doi.org/10.1016/j.minpro.2011.09.002.
[85] A.R. Esquinas, J.I. Álvarez, J.R. Jiménez, J.M. Fernández, Durability of self-compacting concrete made from non-conforming fly ash from coal-fired power plants, Construct. Build. Mater. 189 (2018) 993–1006, https://doi.org/10.1016/j.conbuildmat.2018.09.056.
[86] JCPDS, Joint Committee on Power Diffraction Standard, International Centre for Diffraction, 2003.
[87] S. Luhar, S. Chaudhary, I. Luhar, Thermal resistance of fly ash based rubberized geopolymer concrete, J. Build. Eng. 19 (2018) 420–428, https://doi.org/10.1016/j.jobe.2018.05.025.
[88] E.F. Ledesma, J.R. Jiménez, J. Ayuso, J.M. Fernández, J. De Brito, Maximum feasible use of recycled sand from construction and demolition waste for eco-mortar production - part-I: ceramic masonry waste, J. Clean. Prod. 87 (2015) 692–706, https://doi.org/10.1016/j.jclepro.2014.10.084.
[89] J. Skalny, V. Johansen, N. Ïhaulow, A. Palomo, DEF: una forma de ataque por sulfatos DEF: as a form of sulfate attack, Mater. Construcción 46 (1996) 5–29.
[90] J.M. Fernández, Introducción a Los Cementos, Servicio de Publicaciones de la Universidad de Córdoba, 2004, ISBN 84-7801-731-3.
[91] L.N. Assi, E. Eddie Deaver, P. Ziehl, Effect of source and particle size distribution on the mechanical and microstructural properties of fly Ash-Based geopolymer concrete, Construct. Build. Mater. 167 (2018) 372–380, https://doi.org/10.1016/j.conbuildmat.2018.01.193.
[92] D. Suescum-Morales, Á. Romero-Esquinas, E. Fernández-Ledesma, J. M. Fernández, J.R. Jiménez, Feasible use of colliery spoils as subbase layer for low-traffic roads, Construct. Build. Mater. 229 (2019) 116910, https://doi.org/10.1016/j.conbuildmat.2019.116910.
[93] I.N. Murthy, J.B. Rao, Investigations on physical and chemical properties of high silica sand, Fe-Cr slag and blast furnace slag for foundry applications, Procedia Environ. Sci. 35 (2016) 583–596, https://doi.org/10.1016/j.proenv.2016.07.045.
[94] A.R. Esquinas, C. Ramos, J.R. Jiménez, J.M. Fernández, J. de Brito, Mechanical behaviour of self-compacting concrete made with recovery filler from hot-mix asphalt plants, Construct. Build. Mater. 131 (2017) 114–128, https://doi.org/10.1016/j.conbuildmat.2016.11.063.
[95] D. Suescum-Morales, D. Cantador-Fernández, J.M. Fernández, J.R. Jiménez, The combined effect of CO2 and calcined hydrotalcite on one-coat limestone mortar properties, Construct. Build. Mater. 280 (2020) 122532, https://doi.org/10.1016/j.conbuildmat.2021.122532.
[96] D. Suescum-Morales, J.D. Ríos, A.M.- De La Concha, H. Cifuentes, J.R. Jiménez, J. M. Fernández, Effect of moderate temperatures on compressive strength of ultra-high-performance concrete: a microstructural analysis, Cement Concr. Res. 140 (2021) 106303, https://doi.org/10.1016/j.cemconres.2020.106303.
[97] A.R. Esquinas, E.F. Ledesma, R. Otero, J.R. Jiménez, J.M. Fernández, Mechanical behaviour of self-compacting concrete made with non-conforming fly ash from coal-fired power plants, Construct. Build. Mater. 182 (2018) 385–398, https://doi.org/10.1016/j.conbuildmat.2018.06.094.
[98] A. Gonzalez-Corominas, M. Etxeberria, Properties of high performance concrete made with recycled fine ceramic and coarse mixed aggregates, Construct. Build. Mater. 68 (2014) 618–626, https://doi.org/10.1016/j.conbuildmat.2014.07.016.
[99] W. Ashraf, J. Olek, Elucidating the accelerated carbonation products of calcium silicates using multi-technique approach, J. CO2 Util. 23 (2018) 61–74, https://doi.org/10.1016/j.jcou.2017.11.003.
[100] I.F. Sáez del Bosque, P. Van den Heede, N. De Belie, M.I. Sánchez de Rojas, C. Medina, Carbonation of concrete with construction and demolition waste based recycled aggregates and cement with recycled content, Construct. Build. Mater. 234 (2020) 117336, https://doi.org/10.1016/j.conbuildmat.2019.117336.
[101] X. Ren, L. Zhang, Experimental study of interfacial transition zones between geopolymer binder and recycled aggregate, Construct. Build. Mater. 167 (2018) 749–756, https://doi.org/10.1016/j.conbuildmat.2018.02.111.
[102] J. Xie, J. Wang, R. Rao, C. Wang, C. Fang, Effects of combined usage of GGBS and fly ash on workability and mechanical properties of alkali activated geopolymer concrete with recycled aggregate, Compos. B Eng. 164 (2019) 179–190, https://doi.org/10.1016/j.compositesb.2018.11.067.
[103] J. Wang, J. Xie, C. Wang, J. Zhao, F. Liu, C. Fang, Study on the optimum initial curing condition for fly ash and GGBS based geopolymer recycled aggregate concrete, Construct. Build. Mater. 247 (2020) 118540, https://doi.org/10.1016/j.conbuildmat.2020.118540.
[104] S. Pradhan, S. Kumar, S.V. Barai, Multi-scale characterisation of recycled aggregate concrete and prediction of its performance, Cement Concr. Compos. 106 (2020) 103480, https://doi.org/10.1016/j.cemconcomp.2019.103480.
[105] X.S. Shi, F.G. Collins, X.L. Zhao, Q.Y. Wang, Mechanical properties and microstructure analysis of fly ash geopolymeric recycled concrete, J. Hazard Mater. 237–238 (2012) 20–29, https://doi.org/10.1016/j.jhazmat.2012.07.070.
[106] X.Y. Zhuang, L. Chen, S. Komarneni, C.H. Zhou, D.S. Tong, H.M. Yang, W.H. Yu, H. Wang, Fly ash-based geopolymer: clean production, properties and applications, J. Clean. Prod. 125 (2016) 253–267, https://doi.org/10.1016/j.jclepro.2016.03.019.
[107] S. Hanjitsuwan, S. Hunpratub, P. Thongbai, S. Maensiri, V. Sata, P. Chindaprasirt, Effects of NaOH concentrations on physical and electrical properties of high calcium fly ash geopolymer paste, Cement Concr. Compos. 45 (2014) 9–14, https://doi.org/10.1016/j.cemconcomp.2013.09.012.
[108] F.U.A. Shaikh, Effects of alkali solution on corrosion durability of geopolymer concrete, Adv. Concr. Constr. (2014) 109–123, https://doi.org/10.12989/acc.2014.2.2.109.
[109] P. Nuaklong, V. Sata, P. Chindaprasirt, Influence of recycled aggregate on fly ash geopolymer concrete properties, J. Clean. Prod. 112 (2016) 2300–2307, https://doi.org/10.1016/j.jclepro.2015.10.109.
[110] F. Cartuxo, J. De Brito, L. Evangelista, J.R. Jiménez, E.F. Ledesma, Increased durability of concrete made with fine recycled concrete aggregates using superplasticizers, Materials 9 (2016), https://doi.org/10.3390/ma9020098.
[111] J.R. Jiménez, J. Ayuso, M. López, J.M. Fernández, J. De Brito, Use of fine recycled aggregates from ceramic waste in masonry mortar manufacturing, Construct. Build. Mater. 40 (2013) 679–690, https://doi.org/10.1016/j.conbuildmat.2012.11.036.
[112] J. Temuujin, A. Minjigmaa, B. Davaabal, U. Bayarzul, A. Ankhtuya, T. Jadambaa, K.J.D. Mackenzie, Utilization of radioactive high-calcium Mongolian flyash for the preparation of alkali-activated geopolymers for safe use as construction materials, Ceram. Int. 40 (2014) 16475–16483, https://doi.org/10.1016/j.ceramint.2014.07.157.